Synchronization of endogenous business cycles

Marco Pangallo[1]

[1]Institute of Economics and Department EMbeDS,
Sant'Anna School of Advanced Studies, Pisa 56127, Italy

February 15, 2020

Abstract

Comovement of economic activity across sectors and countries is a defining feature of business cycles. However, standard models that attribute comovement to propagation of exogenous shocks struggle to generate a level of comovement that is as high as in the data. In this paper, we consider models that produce business cycles endogenously, through some form of non-linear dynamics—limit cycles or chaos. These models generate stronger comovement, because they combine shock propagation with synchronization of endogenous dynamics. In particular, we study a demand-driven model in which business cycles emerge from strategic complementarities across sectors in different countries, synchronizing their oscillations through input-output linkages. We first use a combination of analytical methods and extensive numerical simulations to establish a number of theoretical results. We show that the importance that sectors or countries have in setting the common frequency of oscillations depends on their eigenvector centrality in the input-output network, and we develop an eigendecomposition that explores the interplay between non-linear dynamics, shock propagation and network structure. We then calibrate our model to data on 27 sectors and 17 countries, showing that synchronization indeed produces stronger comovement, giving more flexibility to match the data.

Key Words: Synchronization, Business Cycles, Non-linear dynamics, Networks.
JEL Class.: C61 (Dynamic Analysis), C67 (Input-Output Models), E32 (Business Fluctuations, Cycles), F44 (International Business Cycles)

[1]Contact: marco.pangallo@santannapisa.it. I thank Paul Beaudry, Doyne Farmer, Thomas Peron and Alexander Teytelboym for useful comments at various stages of this work. Most of this work is included in two chapters of my DPhil thesis at the Mathematical Institute of the University of Oxford, and was performed while I was also affiliated to the Institute for New Economic Thinking at the Oxford Martin School. I acknowledge funding from Baillie Gifford and from the James S. Mc Donnell Foundation.

1 Introduction

How do different bits of the economy move together? Comovement of economic activity is a defining feature of the business cycle: If fluctuations in different sectors were completely incoherent, we would not observe aggregate business cycles, because booms in some sectors would offset busts in other industries. Comovement across countries is important too, in particular for those countries that are part of monetary unions. Despite its importance, our understanding of what drives comovement is at best limited.

To explain comovement, the literature has largely followed the most popular framework for economic fluctuations. According to this framework, economies would grow smoothly, but fail to do so because they are persistently hit by unpredictable events that originate outside the economy, such as political decisions, natural catastrophes or wars. Within this framework, researchers focused on structure and propagation of these "exogenous" shocks to explain comovement. The literature initially "assumed" comovement, by tracing it back to common shocks hitting several sectors and countries alike (Lucas, 1977). More recent approaches showed that the intricate trade network of intermediate and consumption goods could generate high comovement from shocks that are idiosyncratic to firms or small industries, leading to aggregate fluctuations (Long and Plosser, 1983; Acemoglu et al., 2012; Baqaee and Farhi, 2019). At the international level, scholars have focused on trade and financial linkages (Frankel and Rose, 1998; Imbs, 2006), as well as on multinational corporate control (Cravino and Levchenko, 2017; Di Giovanni et al., 2018), as shock propagators. All these papers only met limited empirical success, in the sense that in most cases they explained no more than a third of the level of comovement that can be found in the data. Kose and Yi (2006) named "trade-comovement puzzle" the inability of models based on trade links and exogenous shocks to generate sufficiently high international comovement.

In this paper, we attack the problem from a different perspective. We challenge the assumption that economies would grow smoothly absent shocks. We follow the "endogenous business cycles" framework, which claims that economies are fundamentally unstable, as fluctuations are at least partially caused by forces internal to the economy. In this framework, the probability of recessions depends on duration of previous expansions (i.e., expansions "die of old age"), although this probability could be far from periodic. Mathematically, economies follow some form of non-linear dynamics—be it limit cycles or chaos. While currently in the minority among macroeconomists, this framework has a long history (Kaldor, 1940) and has recently been gaining new traction (Beaudry et al., 2020). Comovement within the endogenous business cycles framework arises by a combination of shock propagation and alignment, or *synchronization*, of deterministic non-linear dynamics.

Synchronization is a generic property of interacting components of a dynamical system to align their non-linear dynamics in a way that they operate in synchrony, provided some conditions are satisfied. (In this paper, we use the term synchronization in this technical sense, *not* as a synonym of comovement and correlation as usual in economics.) Synchronization is one of the most fascinating phenomena across the natural sciences. It applies to very diverse systems such as oscillating pendula, flashing fireflies, firing neurons, and applauding audiences (Strogatz, 2004).

The economic intuition for why synchronization can help generate higher comovement is as follows. Consider two interacting economic units, say two countries, following some form of non-linear dynamics, such as a limit cycle. On top of that deterministic dynamics, these two countries are hit by idiosyncratic and persistent shock processes. The combination of shocks and deterministic dynamics implies that, at any given time, recessions occur with a certain *probability*. For example, thanks to a series of positive shocks, recessions can be delayed after a peak of the limit cycle has been reached, but recession probability increases as deterministic dynamics move towards the next trough. Because of synchronization, the two countries reach the peak of their deterministic dynamics roughly at the same time. The first country may fall into a recession before the second country because it is hit by a negative shock, while the second country may be enjoying a period of positive shocks. However, the first country would easily drag the second one into a recession, too, because the second country was already predisposed to start a recession anyway.

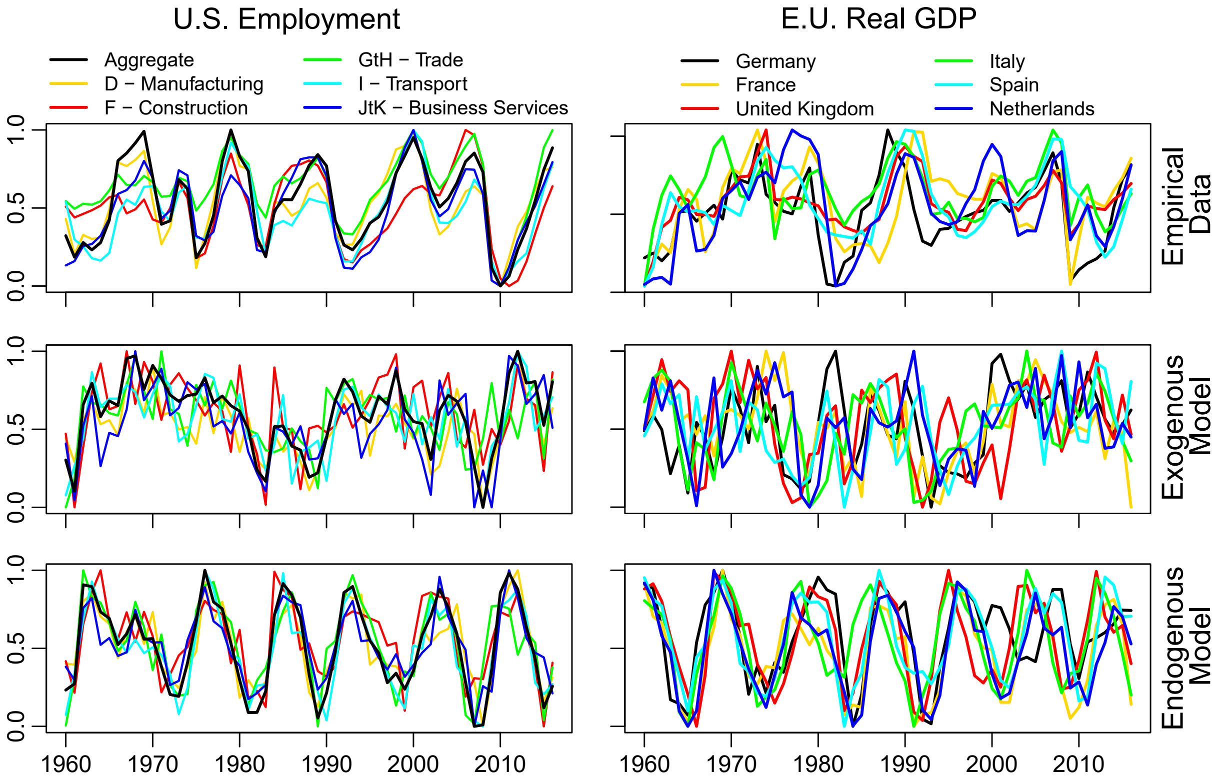

Figure 1: Comparison of empirical and simulated data. In the top panels, we show empirical data from the dataset described in Section 6.1. The top-left panel shows employment data in five large U.S. sectors (ISIC Rev. 3), as well as aggregate employment. The top-right panel shows real GDP in six European countries. All these variables are detrended with a Christiano and Fitzgerald (2003) filter that removes all fluctuations with periodicities above 25 years, and then rescaled between 0 and 1. In the middle and bottom panels, we show simulated data from two realizations of our model. In the middle panels, the model is parameterized so that it would converge to a steady state absent idiosyncratic shocks, and so comovement is caused by shock propagation only. In the bottom panels, we choose parameters so that the model produces limit cycles: comovement is caused by both shock propagation and synchronization. Shocks are identical across the middle and bottom panels.

This intuition is confirmed in Figure 1, where we compare two realizations of our model to empirical data.[1] It is visually clear that the parameterization under which the model generates fluctuations endogenously—complementing idiosyncratic exogenous shocks with limit cycles—produces a level of comovement closer to the data than the parameterization under which fluctuations occur exogenously. Because we keep the shocks identical across the two cases, stronger comovement can only be caused by synchronizing non-linear dynamics. Although this example from a single simulation can obviously be non-representative, we will show that this insight holds in general.

Our goal in this paper is to illustrate how synchronization theory can be useful to explain business cycle comovement. However, the theory that we develop can be applied to explain comovement of any other economic or financial time series, such as commodity, housing and stock prices. To highlight the generality of our approach, we avoid choosing models that focus on specific economic forces causing endogenous business cycles, such as debt dynamics, adaptive expectations, overinvestment or technological progress. We instead adapt the reduced-form model in Beaudry et al. (2020), in which endogenous cycles have more abstract origin. In particular, they are caused by strategic complementarities, that is, the tendency of agents to increase their action if other agents increase their action, too. In macroeco-

[1] We show employment and real GDP for illustration purposes. As we will clarify below, our model produces an abstract indicator of economic activity, so the comparison to employment and GDP should not be taken literally.

nomics (Cooper and John, 1988), this can be thought of as the tendency of firms to increase production if other firms increase production themselves, or the tendency of households to increase consumption if other households in their social network increase consumption, too. This abstract framework can encompass many of the causes for endogenous business cycles listed above.

We first consider a model with abstract agents synchronizing through abstract interaction coefficients. We then specify this model so that agents correspond to sector-country pairs and households, and interaction coefficients correspond to input-output linkages. Importantly, in our input-output model final demand plays a central role, as it influences economic sectors through requirement of consumption goods, but is also influenced by the general performance of the economy. Our demand-driven model stands in contrast with many models of aggregate fluctuations from idiosyncratic shocks (Long and Plosser, 1983; Acemoglu et al., 2012; Baqaee and Farhi, 2019), which focus on supply factors as drivers of fluctuations and comovement.

The analysis of our model yields several novel results. We both use analytical methods and, when this is not possible, extensive numerical simulations. We first illustrate theoretical properties of synchronization, and then move on to the empirical application.

The first part of our theoretical analysis concerns *phase synchronization* (Kuramoto, 2003). This form of synchronization applies to systems exhibiting some form of periodicity, either following limit cycles or low-dimensional chaotic attractors. Assuming that the components of the system would oscillate with different periodicities when isolated, phase synchronization is the alignment of frequencies of oscillation when the components interact. In our business cycle model, we can tune two parameters so as to generate different frequencies of oscillations across agents. We first assess whether phase synchronization can be achieved at all, depending on frequency spread, interaction strength, and structure of the interaction network. We then analyze our input-output specification and find that both the size of a sector (or country) and its interconnectedness in the input-output network determine the power of that sector (or country) to set the common frequency of oscillation—in case a common frequency is achieved. We show that this power, that we name *synchronization centrality*, coincides with the eigenvector centrality of the sector (or country) in a certain normalization of the input-output network. Manufacturing and the U.S. are the sector/country with highest synchronization centrality.

Our theoretical analysis proceeds with a characterization of *complete synchronization*. Under this stronger concept of synchronization, dynamics of all components of the system become perfectly aligned. Because in this paper we study a limit cycle model,[2] if frequencies of oscillation are identical, absent shocks, complete synchronization occurs at all times. However, in our model, agents are hit by idiosyncratic shocks, which act as a desynchronizing factor. Here we extend the master stability function approach (Pecora and Carroll, 1998), which in the original formulation gives a yes/no answer to whether complete synchronization can be achieved, to quantify *how strong* coupling of non-linear dynamics is with respect to idiosyncratic shocks. We show analytically that this depends on structural properties of the interaction network, captured by the eigenvalues and eigenvectors of the normalized Laplacian matrix of the network. Macroeconomists can also view this approach as an eigendecomposition of a generalized impulse response function.

We then analyze more systematically the extent to which synchronization theory can help to empirically explain comovement across sectors and countries. We first calibrate our model to the World Input-Output Database, across 27 sectors and 17 countries, and show that even in the calibrated version of our model endogenous fluctuations always produce stronger comovement than exogenous ones. We then compare the predicted correlations in our model to correlations of employment and GDP empirical data across the same sectors and countries. (This is not the primary focus of our paper and several caveats apply, but we wanted to see how far we could go with this model. Therefore these results should be taken as preliminary.) Endogenous fluctuations do not seem necessary to explain sectoral

[2] All our results apply in the same way if the underlying model was chaotic. In fact, the theory of complete synchronization was initially developed for synchronization of chaos (Pecora and Carroll, 1990).

synchronization within the same country, in the sense that if variance of idiosyncratic shocks is relatively weak, propagation of exogenous shocks produces a level of comovement similar to the one that can be found in the data. However, international synchronization is much better explained by endogenous fluctuations, as in most scenarios exogenous fluctuations produce a level of comovement lower than the one that can be found in the data.

Relation to the literature. This paper is related to several strands of the economics literature. In general, it belongs to the constantly growing stream of papers that investigates how aggregate phenomena originate from behavior at the level of (heterogenous) smaller economic units (Kaplan and Violante, 2018; Dawid and Delli Gatti, 2018). In particular, our model is a disaggregated version of Beaudry et al. (2020), who assume that all agents behave alike and that their interaction network is homogeneous. Our model lets agents behave differently, possibly due to their heterogeneous interaction network. Only when synchronization emerges endogenously we observe aggregate business cycles. In this sense, we contribute to the large literature developing non-linear models of endogenous business cycles,[3] which largely focuses on aggregate variables, without asking if aggregation is justified.

We also contribute to the literatures on sectoral and international comovement. Sectoral comovement originating from idiosyncratic shocks has been investigated at least since Long and Plosser (1983); see also Hornstein and Praschnik (1997) and Cooper and Haltiwanger (1990). A more recent literature studies the origin of aggregate fluctuations from microeconomic shocks (Horvath, 1998, 2000; Acemoglu et al., 2012; Baqaee and Farhi, 2019). While these papers do not explicitly focus on comovement, the emergence of aggregate fluctuations from sectoral shocks implies comovement. The literature studying international comovement is even larger. While many papers are mostly empirical,[4] some papers attempt explaining comovement by building international real business cycle models (Backus et al., 1992). These works generally struggle to obtain a level of comovement that is as high as in the data (Arkolakis and Ramanarayanan, 2009; Johnson, 2014; Liao and Santacreu, 2015), in line with the already mentioned "trade-comovement puzzle" (Kose and Yi, 2006). As already outlined above, we contribute to these strands of literature by showing how synchronization of non-linear dynamics is a powerful way to generate higher comovement, both internationally and within national economies.

We further contribute to the literature on the economics of networks (Carvalho, 2014; Bramoullé et al., 2016). From a microeconomics perspective, our results highlight how different network structures have dramatic effects on synchronization. We also propose an eigenvalue-eigenvector decomposition of shocks on networks that, to the best of our knowledge, is novel in economics. From a macroeconomics perspective, our demand-driven input-output model offers new insights on the structure of the international input-output network. Through the lenses of our model, it is a collection of star networks corresponding to individual countries, which have final demand as their central node (see Figure 12 for an illustration). Manufacturing sectors are the main "bridges" that keep these star networks together, by connecting to manufacturing and final demand in other countries.

Furthermore, this work contributes to the literature on the empirical evidence for non-linear dynamics in economic time series. A first type of evidence could be peaks in spectral density, suggesting existence of limit cycles. Since the work of Granger (1966) this possibility has been disregarded, but Beaudry et al. (2020) show that some U.S. time series produce a clear spectral peak between 9 and 10 years, at lower frequencies than the ones commonly associated to business cycles. More papers have looked for chaos in economic time series,[5]

[3]See, among many others, the contributions and review articles in: Kaldor (1940); Hicks (1950); Goodwin (1951, 1967); Shleifer (1986); Boldrin and Woodford (1990); Foley (1992); Silverberg and Lehnert (1993); Bullard (1994); Matsuyama (2007); Fazzari et al. (2008); De Grauwe (2011); Nikolaidi and Stockhammer (2017).

[4]See, for example, Frankel and Rose (1998); Baxter and Kouparitsas (2005); Imbs (2006); Calderon et al. (2007); Di Giovanni and Levchenko (2010); Ng (2010); Hsu et al. (2011); Kalemli-Ozcan et al. (2013); Cravino and Levchenko (2017); Di Giovanni et al. (2018).

[5]A non-exhaustive list includes Brock (1986); Barnett and Chen (1988); Scheinkman and LeBaron (1989);

but this literature has been unable to provide conclusive evidence (Barnett and Serletis, 2000). Our finding that comovement is better explained by endogenous business cycle models provides indirect support to the existence of non-linear dynamics in economic time series.[6]

Beyond economics, our paper contributes to the literature on synchronization theory (Pikovsky et al., 2003; Arenas et al., 2008; Rodrigues et al., 2016). While several of our results are well-known within the community studying synchronization, some are novel. To the best of our knowledge, for example, the results concerning the importance of different agents in setting the global frequency of oscillations and the extension of the master stability approach are novel contributions to this literature.

Last but not least, we should stress that we are by no means the first who saw the appeal of synchronization theory to explain the origin and comovement of business cycles. Yet, for some reason, the few papers that used synchronization (Haxholdt et al., 1995; Selover and Jensen, 1999; Brenner et al., 2002; Matsuyama et al., 2014; Gualdi et al., 2015) so far had very little impact in macroeconomics. We argue that our work overcomes some limitations of these papers,[7] providing more compelling evidence on the usefulness of synchronization theory within macroeconomics and economics more generally.

Road map. This paper proceeds as follows. In Section 2 we give some background on synchronization theory. In Section 3 we introduce our model of endogenous business cycles, both in its abstract and input-output specifications, and analyze dynamics of homogeneous agents. In Sections 4 and 5 we obtain theoretical results on phase and complete synchronization, respectively. Finally, in Section 6, we compare the predictions of our model to data. Section 7 concludes.

2 Some background on synchronization theory

In a system made by two or more interacting components, synchronization is the adjustment of dynamics of the components due to their interaction. Synchronization was first discovered by Huygens in 1665. He observed that two pendulum clocks hanging from opposite sides of the same wooden beam synchronized their motion in opposite swings. As he correctly noted, this phenomenon was due to the interaction of the two pendula that were imperceptibly moving the beam. The same phenomenon can be observed across a range of natural and social systems. One of the most fascinating manifestations of synchronization is the spontaneous contemporaneous flashing of hundreds of fireflies, which does not need any leader or cue from the environment to occur. Instead, it is sufficient that fireflies adjust their flashing rhythms in response to the flashes of the others. This and many other examples are described in Strogatz (2004).

Why is synchronization so ubiquitous across so diverse systems? It is because all these systems can be described in the common language of dynamical systems theory. It is a generic property of interacting components of a dynamical system to align their non-linear dynamics in a way that they operate in synchrony, provided some conditions are satisfied. In the following, we give some background on the two main approaches in synchronization theory, phase and complete synchronization. (A standard reference for synchronization

Barnett and Serletis (2000); Shintani and Linton (2004); Hommes and Manzan (2006).

[6] Another strand of the empirical literature that our paper contributes to is the one on factor models (Forni and Reichlin, 1998; Foerster et al., 2011). These models find that one or two common factors account for some of the variance of sectoral time series, while idiosyncratic shocks account for the remaining part. Our framework is consistent with these findings, in the sense that the main common factor can be viewed as the synchronizing endogenous cycle.

[7] Our paper (i) uses a general model that can be adapted to several economic circumstances, rather than relying on a specific business cycle model; (ii) studies synchronization on a network of an arbitrary number of agents, rather than just two agents or a trivial topology; (iii) studies complete synchronization, rather than just looking at phase synchronization; (iv) produces "realistic" smooth dynamics, as opposed to dynamics that shows no persistence. Most importantly, we compare the predictions of our model to data, while all other papers are purely theoretical.

theory is Pikovsky et al. 2003. Recent review articles, that include the effect of heterogeneous network structures, are Arenas et al. 2008 and Rodrigues et al. 2016.)

2.1 Phase synchronization

Consider a trajectory $\boldsymbol{X}_t$ of an N-dimensional dynamical system, following an arbitrary limit cycle of period T. Such a trajectory can first of all be characterized by its ordinary frequency $\nu = 1/T$ or angular frequency $\omega = 2\pi/T$. Letting t_0 be a time at which this trajectory is at an arbitrary starting point, it is also possible to characterize it through its phase $\theta(t) = 2\pi(t - t_0)/T \mod 2\pi$, where mod is the modulo operation.

Consider now two trajectories $\boldsymbol{X}_t^1$ and $\boldsymbol{X}_t^2$. They both follow a limit cycle in isolation. They can be characterized by their frequencies ω_1 and ω_2 and by their phases θ_1 and θ_2. Suppose now that the two trajectories become weakly mutually *coupled*, in the sense that the time evolution of $\boldsymbol{X}_t^1$ depends weakly on $\boldsymbol{X}_t^2$, and viceversa. Denote an effective coupling between the two trajectories by K.

When K is greater than the frequency spread $\omega_1 - \omega_2$, the two frequencies converge to a common frequency Ω. The process by which ω_1 and ω_2 become identical is known as *frequency entrainment*. If the two frequencies are identical, $\omega_1 = \omega_2$, also the phases θ_1 and θ_2 become identical. If instead the frequency spread is different from zero, but smaller than K, the two phases keep a constant difference—this is known as *phase locking*. Finally, if the frequency spread is too large or coupling is too weak, phase synchronization may not be achieved. In this case, the frequencies ω_1 and ω_2 remain different, and the phases θ_1 and θ_2 keep changing relative to one another.

Most analytical results for phase synchronization are obtained under relatively strong simplifying assumptions. For example, a common technique known as *phase reduction theory* (Pikovsky et al., 2003; Nakao, 2016) makes it possible to approximate the motion of each trajectory and the effect of coupling by a simple phase description of the dynamics. This approximation is only possible when coupling is weak and mostly the phase is affected by coupling (i.e., coupling has negligible effects on the amplitude of fluctuations). Although these simplifying assumptions do not hold for the system that we study, we will show that many of our results are in line with well-known results in phase synchronization theory.

Finally, while so far we have been assuming that $\boldsymbol{X}_t^1$ and $\boldsymbol{X}_t^2$ follow deterministic limit cycles, we stress that all properties discussed so far also hold for systems that do not exhibit perfect periodicity. These include low-dimensional chaotic systems and limit cycles perturbed with relatively weak noise. The theory that extends phase synchronization to these systems treats perturbations to periodicity as stochastic noise terms in the phase equations—for more details, see Rosenblum et al. (1996) and Chapters 9 and 10 in Pikovsky et al. (2003).

2.2 Complete synchronization

Phase synchronization is a relatively weak synchronization concept, as it only involves the frequency and phase of trajectories. Oscillations are also characterized by other variables, such as their amplitude. Moreover, in case of relatively high-dimensional chaotic dynamics that do not exhibit any clear periodicity, there is no sense in which focusing on frequency and phase is useful. Complete synchronization is both a stronger and more general synchronization concept: It is the property of dynamics of different components of the system to become perfectly aligned.

The concept of complete synchronization was developed to study synchronization of chaos (Pecora and Carroll, 1990). It considers a set of identical oscillators following some chaotic dynamics starting from very similar initial conditions (from a "synchronized state"). Although the exponential divergence of trajectories acts as desynchronizing factor, coupling works in the opposite direction. Complete synchronization theory quantifies the balance between synchronizing and desynchronizing factors by computing certain types of Lyapunov exponents. In case coupling is strong enough, relative to dimensionality of chaos, the synchronized state is stable, and trajectories remain perfectly aligned at all times.

In its original formulation, complete synchronization was concerned with identical deterministic chaotic oscillators. However, the same insights hold for slightly different oscillators, or for oscillators hit by (weak) noise.

This theory has extensively been used to assess the synchronizability of complex interaction networks (Pecora and Carroll, 1998; Barahona and Pecora, 2002; Arenas et al., 2008). In Section 5 we will build on complete synchronization to develop a theory that accounts for synchronization of non-linear dynamics, noise propagation and interaction structure. We will explain complete synchronization technically at that point.

3 A general framework for endogenous economic fluctuations

Over decades, researchers proposed many economic forces as possible generators of endogenous business cycles. (For some references, see footnote 3.) Some scholars focused on the role of finance, others on real factors such as investment and inventories, still others on bounded rationality and adaptive expectations. Even more forces have been proposed, including overlapping generations effects, preference switching, search and matching, technological progress, and wage bargaining. To discuss synchronization of endogenous business cycles, it would be limiting to focus on a particular economic force, as results could heavily depend on this choice. It would be desirable to use a macroeconomic framework that is as general as possible.

Luckily, Beaudry et al. (2015) have recently proposed such a framework.[8] The authors focus on strategic complementarities (Bulow et al., 1985; Cooper and John, 1988) between agents as the main force leading to endogenous cycles. In their framework, decisions of the agents self-reinforce through interactions, leading to an instability of the steady state, but at some point implosive forces set in that prevent dynamics from exploding. Many of the narratives for endogenous business cycles listed above can be cast within this framework, as will be clarified below.

Here we present a slightly modified version of the model in Beaudry et al. (2015), letting decisions and the interaction network be heterogeneous across agents. In this section, we start introducing the model in an abstract interaction network, we then consider a specification of the model in which the interaction network is represented by a "generalized" input-output network, and finally analyze dynamics in a homogeneous case.

3.1 Abstract interaction network

Consider N agents, indexed by $i \in \mathcal{I} = \{1, \dots, N\}$. Denote by x^i an accumulation variable representing a stock of agent i, and by y^i a decision variable representing a flow. We can think of y as level of production and of x as level of inventories; we can also think of y as level of investment or consumption of durable goods, and of x as capital or net worth, respectively.

The time evolution of accumulation variable x^i is simple. At each time step t, it depreciates by a factor δ, and increases by the decision variable y^i_t. In formula, $x^i_{t+1} = (1-\delta)x^i_t + y^i_t$. Consider for example the interpretation of x as capital (machinery) and of y as investment. At every time step, capital depreciates, due to obsolescence and wear and tear in production. At the same time, old machinery is replaced by an amount of new machinery corresponding to investment y^i_t. The other interpretations for x and y lead to similar narratives. If x is the stock of inventories and y is production, new goods are added to the stock of inventories (and then potentially shipped to customers from there). If x is consumption of durable goods, such as cars or houses, and y is net worth, purchasing durable goods adds to one's personal wealth.

[8] Here we reference the initial working paper (Beaudry et al., 2015), rather than the final journal version (Beaudry et al., 2020), because it specifies this general framework in greater detail.

The dynamics of the decision variable y^i depends instead on the interactions among agents. We first write the formula for the evolution of y^i, and then explain the various terms: $y^i_{t+1} = \alpha^i_0 + \alpha^i_1 x^i_t + \alpha^i_2 y^i_t + F\left(\overline{y}^i_t\right)$.[9] The planned level of y for agent i, y^i_{t+1}, depends on the current level of y, y^i_t, the current level of x, x^i_t, and, most importantly, on a term $\overline{y}^i_t$, capturing the interactions among the decision variables y of the agents. The effect of this latter variable is mediated by a function $F(\cdot)$, which will be explained below. The interaction term $\overline{y}^i_t$ is defined as $\overline{y}^i_t = \epsilon^i_i y^i_t + \sum_{j=1}^N \epsilon^i_j y^j_t$, where $\epsilon^i_j \in [0,1]$, such that $\sum_j \epsilon^i_j = 1$. Each term ϵ^i_j, which can be thought of as an *interaction coefficient*, is the weight that the decision variable of agent j has in determining the value of $\overline{y}^i_t$. This of course includes the weight ϵ^i_i that the own decision variable of agent i has in setting $\overline{y}^i_t$. The values of ϵ^i_j, for all i and j, define a weighted, directed, interaction network.

The function $F(\cdot)$, is a non-linear function that determines the effect of interactions. When the decision variables of the agents with whom agent i interacts increase, so that $\overline{y}^i_t$ becomes larger, if agent i raises her own decision variable, $y^i_{t+1} > y^i_t$, one says that there are *strategic complementarities* between agent i and the agents with whom she interacts (Cooper and John, 1988). If instead, due to an increase of $\overline{y}^i_t$, agent i reduces her decision variable, $y^i_{t+1} < y^i_t$, one talks about *strategic substitutability*. We will choose the function $F(\cdot)$ so that, depending on the value of $\overline{y}^i_t$, our model will encompass both the complementarity and substitutability regimes. What will generate cyclical behavior in this model is the continuous switching between the two regimes (Beaudry et al., 2015). (See Section 3.3.)

We now complete the description of the model. We first assume that the dependence of the planned level of y for agent i, y^i_{t+1}, on y^i_t and x^i_t, is linear and dependent on two parameters α^i_1 and α^i_2. We take α^i_1 to be negative, and α^i_2 to be positive and bounded between zero and one. These assumptions reflect decreasing returns to accumulation, i.e. willingness to avoid excessive stocks of inventories, capital or net worth, and sluggishness in the adjustment of the decision variable, i.e. difficulty to quickly modify the level of production, investment, or consumption of durable goods. The first assumption will be instrumental for the switching between regimes of strategic complementarity and substitutability, the second assumption will be useful to introduce smoothness in the dynamics.[10] Importantly for our analysis of synchronization, we let α^i_1 and α^i_2 be heterogeneous across agents. This means that some agents dislike accumulation more than others, and some agents have more difficulty than others in adjusting their decision variables. These differences will generate heterogeneous frequencies of oscillation across agents.

We finally add two noise terms u^i_t and v_t to the evolution of the decision variables, corresponding to exogenous shocks. The first noise term is idiosyncratic to each agent, while the second term is common across agents. Both terms are AR(1) processes. This means that idiosyncratic shocks evolve as $u^i_{t+1} = \rho_u u^i_t + \iota_t$, where $\rho_u \in [0,1]$ is a persistence parameter and ι^u_t is white noise normally distributed with mean zero and standard deviation σ_u. The common shock evolves similarly, $v_{t+1} = \rho_v v_t + \iota^v_t$, where ι^v_t is the same white noise process, but with standard deviation σ_v.

Our model for endogenous business cycles is thus fully specified by the following equations, for all agents i:

$$\begin{aligned} & x^i_{t+1} = (1-\delta)x^i_t + y^i_t, \\ & y^i_{t+1} = \alpha^i_0 + \alpha^i_1 x^i_t + \alpha^i_2 y^i_t + F\left(\overline{y}^i_t\right) + u^i_t + v_t, \\ & \overline{y}^i_t = \epsilon^i_i y^i_t + \textstyle\sum_{j=1}^N \epsilon^i_j y^j_t, \quad \epsilon^i_j \in [0,1], \quad \sum_j \epsilon^i_j = 1, \\ & F(y) = \beta_0 + \beta_1 y + \beta_2 y^2 + \beta_3 y^3 + \beta_4 y^4. \end{aligned} \tag{1}$$

The last equation represents our arbitrary choice for $F(\cdot)$, that we parameterize as a generic

[9] A minor difference with respect to Beaudry et al. (2015) is that y^i_{t+1} depends only on variables at t, while in Beaudry et al. (2015) it depended on both variables at t and (contemporaneous) variables at $t+1$. As there did not seem to be much difference in the implied dynamics, we chose this form as it was computationally simpler. Economically, it corresponds to assuming that the decision variables of the agents with whom agent i interacts have a lagged effect on her decision.

[10] A problem of many endogenous business cycle models is that they generate a "sawtooth" dynamics that has no persistence, in stark contrast to empirical time series.

quartic function (Beaudry et al., 2015). The choice of a quartic rather than another functional form is not important, to the extent that $F(\cdot)$ can be parameterized as will be described in Section 3.3.

In the case in which all parameters α_0^i, α_1^i, and α_2^i are identical across agents i, all interaction coefficients ϵ_j^i are identical and equal to $1/N$ (complete and homogenous interaction network), and all agents behave alike, $x_t^i = x_t^j$ and $y_t^i = y_t^j$, for all agents i and j and for all times t (which implies no idiosyncratic shocks u_t^i), equations (1) exactly recover the model in Beaudry et al. (2015). Our assumptions on agents' heterogeneity implies that agents may or may not synchronize their behavior and so increase (or decrease) their decision variables at the same time. If they synchronized their behaviors, agents would produce aggregate business cycles but, if they did not, an aggregate business cycle would not emerge, because their decision variables would generally cancel out.

3.2 Input-output specification

Although an agent in the model presented in Section 3.1 could be an individual firm or household, in this paper we consider some level of aggregation. In particular, we think of agents as economic sectors (industries) across countries, the basic unit of analysis being a sector-country pair.[11] What should interaction coefficients between sector-country pairs represent?

A large literature has dealt with the identification of economic factors that lead to comovement of economic activity across sectors and countries. Aggregate shocks, both at the national and international level, have initially been pointed out as an obvious possible cause for synchronization (Lucas, 1977). Other researchers proposed trade linkages—of intermediate, investment and consumption goods—to also explain synchronization both at the national and international level (Long and Plosser, 1983; Hornstein and Praschnik, 1997; Foerster et al., 2011; Frankel and Rose, 1998). Moreover, national synchronization could be caused by consumption good complementarities (Cooper and Haltiwanger, 1990): Because consumers are also workers, if things go well within a sector and workers in that sector get a pay increase, they will also be able to spend on consumption goods from other sectors, leading to positive comovement. International synchronization, furthermore, could be induced by similar industrial structures, to the extent that exogenous shocks are sector-specific (Imbs, 2004). Finally, the role of financial linkages is less clear, as on average financial linkages seem to lead to *less* synchronization (Kalemli-Ozcan et al., 2013).

In the following, we present an adaptation of the model presented in Section 3.1 that can encompass several of the factors above, namely common shocks (e.g. fiscal and monetary policy), trade linkages, consumption good complementarities and similar industrial structure. To achieve this goal, the interaction network in our adaptation is the international input-output network including final demand, and sector-country pairs can be hit by country-specific, sector-specific and sector-country-specific shocks.

We denote sector-country pair "agents" by ij, where i indicates sectors, $i \in \mathcal{I} = \{1, \dots, I\}$, and j denotes countries $j \in \mathcal{J} = \{1, \dots, J\}$. We also consider J final demand nodes, denoted by $0j$, i.e. $i = 0$ and $j \in \mathcal{J} = \{1, \dots, J\}$, so that the total number of agents is $N = (I + 1) \cdot J$. When considering firms in sector-country pairs, we can think of the decision variable y as production, and of the accumulation variable x as inventories. We think of final demand as being fully based on consumption goods,[12] so that the final demand node in a given country is entirely "composed" of households within that country. Under

[11] An alternative choice could be region(state)-country pairs, but the relatively higher amount of data on sectors made us choose sectors. Considering regions would be an interesting extension for future work.

[12] We do not consider investment as a component of final demand for two reasons. First, although it is more volatile than consumption, its share of final demand is only around 20%. Second, while there are abundant data on the intersectoral flow of intermediate goods, there are no systematic data of the intersectoral flow of capital goods (see vom Lehn and Winberry 2019 for an interesting new paper that tries to reconstruct the investment network for the US economy). Additionally, we model government in an abstract way through country-specific aggregate shocks, without explicitly considering final demand by the government.

such interpretation, the final demand interpretation of y can be consumption, while x can be interpreted as wealth.

One first challenge for the adaptation of the model is to account for the diverse size of sector-country pairs. To do so, we think of x_t^{ij} and y_t^{ij} as "intensive" variables fluctuating about their steady state value. In parallel, we consider "extensive" variables $X_t^{ij} = O^{ij} x_t^{ij}$ and $Y_t^{ij} = O^{ij} y_t^{ij}$, where O^{ij} is a constant[13] representing total output of sector-country pair ij, for $i \in \{1, \ldots, I\}$, or total demand in country j, for $i = 0$. We choose parameters so that there exists a unique steady state denoted by $y_s^{ij} = 1$, so that, at the steady state, production of sector i in country j is indeed given by $Y_s^{ij} = O^{ij}$, and total final demand in country j is $Y_s^{0j} = O^{0j}$.

We now first consider the evolution of sector-country pair nodes, and after that we discuss final demand nodes. The evolution of intensive accumulation and decision variables x^{ij} and y^{ij} is analogous to the general specification in Eq. (1). In the following, we specify the interaction term. For $i > 0$, steady-state total output of sector-country pair ij is defined as $O^{ij} := \sum_{k=0}^{I} \sum_{l=1}^{J} W_{kl}^{ij}$, with W_{kl}^{ij} being the value of the flow of goods and services from sector-country ij to sector-country kl or final demand $0l$ in the steady state. The coefficients W_{kl}^{ij} can directly be read off international input-output tables (we assume the input-output network fixed over time). Total demand received by sector-country pair ij at time t is obtained by multiplying the steady-state value flows W_{kl}^{ij} by the intensive variables y_t^{kl} (including $kl = ij$),

$$\overline{Y}_t^{ij} = W_{ij}^{ij} y_t^{ij} + \sum_{\substack{k=0 \\ k \neq i}}^{I} \sum_{\substack{l=1 \\ l \neq j}}^{J} W_{kl}^{ij} y_t^{kl}. \tag{2}$$

We define the interaction term $\overline{y}_t^{ij}$ as intensive total demand received by sector ij, given by

$$\overline{y}_t^{ij} := \overline{Y}_t^{ij} / O^{ij} = w_{ij}^{ij} y_t^{ij} + \sum_{\substack{k=0 \\ k \neq i}}^{I} \sum_{\substack{l=1 \\ l \neq j}}^{J} w_{kl}^{ij} y_t^{kl}, \tag{3}$$

with $w_{kl}^{ij} := W_{kl}^{ij} / O^{ij}$. Given the definition of O^{ij}, $\sum_{k=0}^{I} \sum_{l=1}^{J} w_{kl}^{ij} = 1$; this means that the dynamics of sector-country pairs are identical to the ones of agents in Eq. (1), with the interaction structure specified by the input-output coefficients w_{kl}^{ij}.

An important point is that the input-output coefficients w_{kl}^{ij}, normalized "by row", are different from the technical coefficients of input-output analysis, which are rather normalized "by column" (Miller and Blair, 2009). Technical coefficients are widespread in economics, and are for example used in the literature on aggregate fluctuations from idiosyncratic shocks (Horvath, 2000; Acemoglu et al., 2012; Baqaee and Farhi, 2019). Why do we use different coefficients? The reason is that models using technical coefficients are focused on *supply.* This makes sense, for example, in models of disruptions along value chains: if suppliers are unable to provide the required necessary intermediate good, firms have to cut back on production. Our model is instead *demand-driven.*[14] Using the same analogy, if customers demand less goods, firms cut back on production. While the debate about demand-driven and supply-driven models is unresolved in economics, we find the demand-driven specification more meaningful to model fluctuations based on strategic complementarities.

We now consider the evolution of final demand nodes. As for sector-country pairs, accumulation and decision variables evolve like in the general framework. The interaction term, however, is different. We assume that households, which in our specification fully determine final demand, work in the various sectors of the economy within their country, proportionally to the size of these sectors. Final demand then depends on the cyclical

[13]Our model does not consider growth. We could easily include a constant growth trend, but it would be an obvious extension with minor value added. It would be more interesting to explore the interaction between cyclicality and growth (Matsuyama, 1999), but we consider that out of the scope of the present paper.

[14]This implies that shocks propagate upstream, in contrast with the models above in which shocks propagate downstream.

movements of sectors, weighted by their size. This is meant to capture the idea that sectors that are not doing well may lay off workers or reduce their wages, depressing final demand of those workers. Therefore,

$$\overline{y}_t^{0j} := \frac{1}{O^j} \sum_{i=1}^{I} O^{ij} y_t^{ij}, \quad O^j := \sum_{i=1}^{I} O^{ij}. \tag{4}$$

In network terms, final demand is just a node whose out-going edges are proportional to the out-strengths of the pointed nodes. An example of all interaction coefficients, including both input-output and final demand ones, will be given in Table 1.

Finally, we allow for sector-country-specific shocks u_t^{ij}, sector-specific shocks v_t^i, and country-specific shocks z_t^j, all autoregressive processes of order one, with parameters ρ_u, σ_u, ρ_v, σ_v, and ρ_z, σ_z, respectively.

Summing up, the input-output specification of the endogenous business cycle model described in Section 3.1 is given by the following equations, for all $i \in \{0, \dots I\}$ and $j \in \{1, \dots, J\}$:

$$\begin{aligned}
&x_{t+1}^{ij} := X_{t+1}^{ij}/O^{ij} = (1-\delta) x_t^{ij} + y_t^{ij}, \\
&y_{t+1}^{ij} := Y_{t+1}^{ij}/O^{ij} = \alpha_0^{ij} + \alpha_1^{ij} x_t^{ij} + \alpha_2^{ij} y_t^{ij} + F\left(\overline{y}_t^{ij}\right) + u_t^{ij} + v_t^i + z_t^j, \\
&\overline{y}_t^{ij} := \overline{Y}_t^{ij}/O^{ij} = w_{ij}^{ij} y_t^{ij} + \textstyle\sum_{\substack{k=0 \\ k \neq i}}^{I} \sum_{\substack{l=1 \\ l \neq j}}^{J} w_{kl}^{ij} y_t^{kl}, \quad i \in \{1, \dots, I\}, \\
&\overline{y}_t^{0j} := \tfrac{1}{O^j} \textstyle\sum_{i=1}^{I} O^{ij} y^{ij}, \quad O^j := \sum_{i=1}^{I} O^{ij}, \\
&F(y) = \beta_0 + \beta_1 y + \beta_2 y^2 + \beta_3 y^3 + \beta_4 y^4.
\end{aligned} \tag{5}$$

This stylized model captures most of the channels that previous research found were useful to explain comovement. In terms of sectoral comovement within the same country j, it captures (i) national shocks through the common noise term z_t^j; (ii) trade of intermediate goods through the input-output network coefficients w_{kj}^{ij}, for $i > 0$; (iii) final demand linkages through the weight O^{ij}/O^j that each sector has in determining the evolution of final demand. In terms of international comovement, the model captures (i) international trade of final and intermediate goods, disaggregated by sector, through the input-output coefficients w_{kl}^{ij}, for $j \neq l$; (ii) similarity in industrial structure, through sector-specific shocks v_t^i; (iii) common fiscal and monetary policy, by correlating national shocks z_t^j across a subset of countries. Given its richness and parsimony, this very simple model seems an ideal choice to illustrate the mechanisms for synchronization of endogenous business cycles across sectors and countries.

3.3 Dynamics of homogeneous agents

Here we mathematically describe and build some intuition into how this general framework for endogenous fluctuations may generate cyclical dynamics (see Beaudry et al. 2015 for more details). For simplicity, we consider the case of the abstract interaction network in Section 3.1. We focus on a single agent i whose dynamics is purely driven by her own decision variable, namely $\epsilon_i^i = 1$, $\epsilon_j^i = 0$, for all $j \neq i$. This assumption is mathematically equivalent to the situation in which the interaction network is homogenous and all agents behave alike, as in Beaudry et al. (2015).[15]

We first look for the steady state (x_s^i, y_s^i). Following the discussion in Section 3.2, we constrain parameters so that $y_s^i = 1$ is the unique steady state. Noting that the steady state value of the accumulation variable is $x_s^i = y_s^i/\delta$, for $y_s^i = 1$ to be a steady state the following relation must hold: $\alpha_0^i = 1 - \alpha_1^i/\delta - \alpha_2^i - F(1)$. In the following, we always select

[15]Interactions "with themselves" and interactions with other, homogeneous, agents are not conceptually equivalent, to the extent that strategic complementarities originate only from interactions with other agents. However, the two situations can be made conceptually equivalent either by assuming that strategic complementarities can also originate within the same agent (e.g. increasing returns in firm production) or by assuming that each agent is "composed" of many other agents—e.g., a sector depending on itself can be viewed as homogeneous firms within that sector interacting with one another.

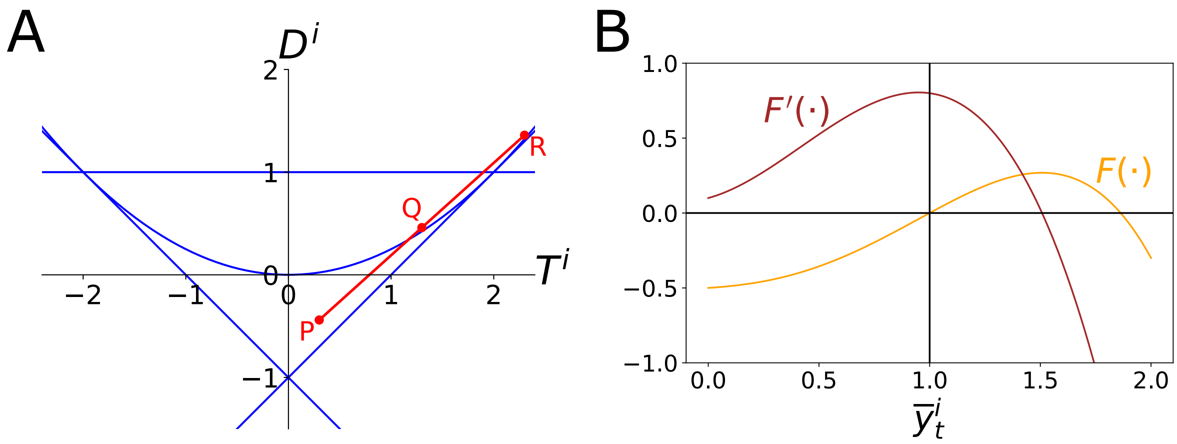

Figure 2: Stability of dynamics for homogeneous agents. (A) Diagram for stability of 2-dimensional maps. The blue lines correspond to $D^i = 1$, $D^i = T^i - 1$, $D^i = -T^i - 1$ and $D = (T^i)^2/4$. The red line corresponds to varying $F'(1)$ with the other parameters fixed. (B) Function $F(\cdot)$ and its first derivative $F'(\cdot)$ for $\bar{y}^i_t \in [0, 2]$.

α^i_0 so that this condition is satisfied. For the steady state to be unique, the slope of the line $-\alpha^i_0 + y^i_t(1 - \alpha^i_1/\delta - \alpha^i_2)$ must be larger than the derivative of F at $y^i_s = 1$, namely

$$1 - \alpha^i_1/\delta - \alpha^i_2 > F'(1). \tag{6}$$

The Jacobian of this system is

$$\mathcal{J} = \begin{pmatrix} 1-\delta & 1 \\ \alpha^i_1 & \alpha^i_2 + F'(1) \end{pmatrix}. \tag{7}$$

Stability of the steady state is completely characterized in terms of the trace $T^i = 1 - \delta + \alpha^i_2 + F'(1)$ and determinant $D^i = (1-\delta)\left(\alpha^i_2 + F'(1)\right) - \alpha^i_1$ of the Jacobian. Following the standard conditions for 2-dimensional maps, stability obtains if $D^i < 1$, $D^i > T^i - 1$ and $D^i > -T^i - 1$. If $D^i > (T^i)^2/4$, the eigenvalues of the Jacobian are complex, and so the system admits either damped oscillations or sustained cycles. If the line $D^i = 1$ is crossed above $D^i = (T^i)^2/4$, the system undergoes a Hopf (Neimark-Sacker) bifurcation.[16]

To build some intuition into the transition between stability and instability, in Figure 2A we plot the usual diagram for the stability of 2-dimensional maps. We set the parameters $\alpha^i_2 = 0.4$, $\alpha^i_1 = -0.1$, $\delta = 0.1$, and vary $F'(1)$ in the interval $F'(1) \in [-1, 1]$.[17] In other words, we consider the level of complementarity or substitutability at the steady state as a bifurcation parameter. Point P corresponds to $F'(1) = -1$. This corresponds to strategic substitutability, and indeed under this parameterization the steady state is a stable node, meaning that eigenvalues are real and of magnitude smaller than one. Point Q corresponds to $F'(1) = 0$, i.e. to a transition between strategic complementarity and substitutability. Under these parameters, the system has a stable focus, with complex eigenvalues of magnitude smaller than one. As the level of complementarities increases, the steady state loses stability through a Hopf bifurcation, up to point R, corresponding to $F'(1) = 1$.

The analysis so far has focused on local stability of the steady state. To build some intuition into global dynamics, in Figure 2B we plot the function $F(\cdot)$ and its first derivative. Here, and throughout, we follow Beaudry et al. (2015) and select $\beta_0 = -0.5$, $\beta_1 = 0.1$, $\beta_2 = 0.2$, $\beta_3 = 0.5$ and $\beta_4 = -0.3$. This choice guarantees that the function F is increasing at $\bar{y}^i_t = 1$ and decreasing when $\bar{y}^i_t$ becomes large, guaranteeing the existence of a regime of strategic substitutability that prevents explosive dynamics.[18]

[16]Beaudry et al. (2015) show that the Hopf bifurcation is supercritical, i.e. the resulting limit cycle is attractive. While the dynamical system that we consider is slightly different (see footnote 9), numerical simulations indicate that the Hopf bifurcation is indeed supercritical.

[17]The uniqueness condition (6) is satisfied for all these values of $F'(1)$.

[18]This choice of parameters also yields, conveniently, $F(1) = 0$.

Starting from a situation below the steady state, the regime of strategic complementarity makes it optimal for agent i to increase her decision variable y^i, in a way that she overshoots the steady state. Explosive economic forces are at play. However, as agent i starts to overaccumulate, because the value of y^i more than offsets the depreciation $(1-\delta)x^i$, due to the negativity of the parameter α_1^i the rise of y^i slows down. Moreover, as y^i increases, the regime of strategic substitutability sets in, corresponding to implosive economic forces. Soon, y^i reverts and starts to decrease. At some point, the decrease in y^i will bring back to a regime of strategic complementarity, making agent i increase her decision variable again, and the process restarts.

Depending on the interpretation for the accumulation variable x, the decision variable y, and the function F, the narrative based on the switching between strategic complementarity and substitutability regimes could correspond to several economic forces causing endogenous business cycles. Beaudry et al. (2020), for example, consider a microfounded model in which x is net worth, y is consumption of durable goods, and F models banks' willingness to give loans. In good times, lending is perceived safe, and so agents can borrow to consume more durable goods. This further strengthens the economic boom, making lending to be perceived even safer (strategic complementarity). When the economy slows down because of overaccumulation, lending instead starts to be perceived less safe, making banks cut back on credit (strategic substitutability). This behavior of banks can easily trigger a recession, which lasts until agents have liquidated assets in excess, at which point the cycle starts again. The narrative in Beaudry et al. (2020) is similar to many of the narratives for finance-based endogenous business cycles. However, the strategic complementarity-substitutability framework easily lends itself to other narratives, such as ones based on overinvestment in the Keynesian tradition (Kaldor, 1940; Hicks, 1950; Goodwin, 1951), and ones based on temporal clustering of technological innovations (Judd, 1985; Shleifer, 1986; Matsuyama, 1999).

A last question concerning the dynamics of uncoupled/homogeneous agents is about how α_1^i and α_2^i determine the frequency of oscillation, in case the steady state is unique and unstable. For the following calculation, we drop the superscripts i. The eigenvalues are obtained from the trace T and determinant D of the Jacobian from the standard formula

$$\lambda_{1,2} = \frac{T}{2} \pm \sqrt{\left(\frac{T}{2}\right)^2 - D}. \tag{8}$$

In the region of the parameter space that we are interested about, the eigenvalues are complex, $D > T^2/4$. Denoting the negative argument of the square root on the right hand side in Eq. (8) by $M = -\left[(T/2)^2 - D\right]$, $M > 0$, the eigenvalues can also be written $\lambda_{1,2} = T/2 \pm i\sqrt{M}$, where i here denotes the imaginary unit. The frequency of oscillation is approximated by the argument ψ of the eigenvalues, $\psi = \arctan \operatorname{Im}\lambda / \operatorname{Re}\lambda = \arctan \sqrt{M}/(T/2)$. To calculate the effect of α_1 and α_2 on the frequency, we thus calculate the derivative of ψ with respect to these parameters. Starting from α_1,

$$\frac{\partial \psi}{\partial \alpha_1} = \frac{1}{1 + M/(T^2/4)} \cdot \frac{1}{T/2} \cdot \frac{1}{2\sqrt{M}} \cdot \frac{\partial M}{\partial \alpha_1}. \tag{9}$$

The first and third term on the right hand side are always positive. For the parameters that yield an unstable steady state the trace T is always positive, so also the second term is always positive. The last term is $\partial M/\partial \alpha_1 = -1$. Therefore, $\partial \psi/\partial \alpha_1 < 0$. Because we restricted $\alpha_1 < 0$, this means that values of α_1 that are larger in absolute value increase ψ. The economic interpretation is that a stronger dislike for accumulation increases the frequency, all else equal.

We now consider the effect of α_2:

$$\frac{\partial \psi}{\partial \alpha_2} = \frac{1}{1 + M/(T^2/4)} \cdot \frac{\frac{1}{2\sqrt{M}} \cdot \frac{\partial M}{\partial \alpha_2} \cdot \frac{T}{2} - \frac{\sqrt{M}}{2}}{T^2/4} = \frac{T\frac{\partial M}{\partial \alpha_2} - 2M}{(1 + M/(T^2/4))T^2\sqrt{M}}. \tag{10}$$

In the above equation, all terms in the denominator are always positive. We calculate

$$\frac{\partial M}{\partial \alpha_2} = \frac{1 - \delta - \alpha_2 - F'(1)}{2}. \tag{11}$$

For $\alpha_2 > 1 - \delta - F'(1)$, as is the case for the parameters we choose, this derivative is always negative, making the numerator on the right hand side on Eq. (10) negative (recall that $T > 0$ and $M > 0$). Therefore, $\partial\psi/\partial\alpha_2 < 0$. Since we restricted α_2 to take positive values, an increase of α_2 in absolute value leads to a decrease of ψ. In economic terms, all else equal, high adjustment costs lead to slower and smoother dynamics.

The difference in frequency due to different parameters α_1^i and α_2^i induces heterogeneous oscillations across agents. What can we expect in terms of business cycles? We are going to look at that in the next section.

4 Phase synchronization

We now couple agents and analyze how their frequencies of oscillation may—or may not—entrain. In Section 4.1 we study the generic business cycle model in Eq. (1) on an abstract interaction network. Some simplifying assumptions on the interactions make it easy to understand the effect of the topology of the network. In Section 4.2 we analyze the input-output model (Eq. 5) on the empirical input-output network, making it possible to derive insights on the sectors and countries that have most power in determining the common frequency of oscillation. All results in this section are obtained by numerical simulations, because analytical methods for phase synchronization require strong simplifying assumptions.

4.1 Abstract interaction network

We consider a special interaction network for which $\epsilon_j^i := \epsilon/k_i$ if j is connected to i and $j \neq i$, where k_i is the number of nodes i is connected to (degree of i). From the normalization condition it follows that $\epsilon_i^i = 1 - \epsilon$. This parameterization makes it possible to focus on the topology of the network. For simplicity, we further assume that the network is undirected, that is, if i is connected to j, also j is connected to i. The parameter ϵ makes it possible to quantify how much each node depends on the others. The larger ϵ, the stronger the dependence on the others. If $\epsilon = 0$, the dynamics of each node is independent from the others, and corresponds to the one described in Section 3.3. We study a setting with $N = 10$ agents.

We select parameters so that all agents of the uncoupled system fluctuate, and study the effect of coupling on the entrainment of the various frequencies of oscillation.[19] We fix $\delta = 0.1$, $\alpha_2^i = 0.4$ for all agents i, and vary α_1^i.[20] Agents whose dislike for accumulation α_1^i is stronger (in absolute value), when uncoupled, oscillate with higher frequency.

Deterministic cycles. We first analyze the case in which the noise terms in Eq. (1) are set to zero. The produced dynamics is clearly at odds with real-world business cycles, which are not perfectly periodic. However, a deterministic assumption is useful as an approximation and, as we show at the end of this section, synchronization results are robust to introducing some noise. Cycles augmented with relatively small noise are perfectly consistent with the U.S. business cycle (Beaudry et al., 2020).

We give some intuition on the effect of coupling on dynamics in Figure 3. Here, we assign a distinct value of α_1^i to each agent by evenly spacing the interval $\alpha_1^i \in [-0.1, -0.02]$. In

[19]It is also interesting to study what happens in terms of stability when coupling stable and unstable dynamics. We find that small values of coupling tend to make stable agents unstable, but, as coupling strength increases, dynamics of all agents tend to become stable. The topology of the network has interesting effects: for example, the central node of a star network has more power in making the system stable or unstable, depending on its own stability. We do not report these results here as our focus is on synchronization.

[20]The results would be equivalent if we kept α_1^i fixed and varied α_2^i, to the extent that the frequencies produced were the same. We vary α_1^i because it produces a wider range of frequencies.

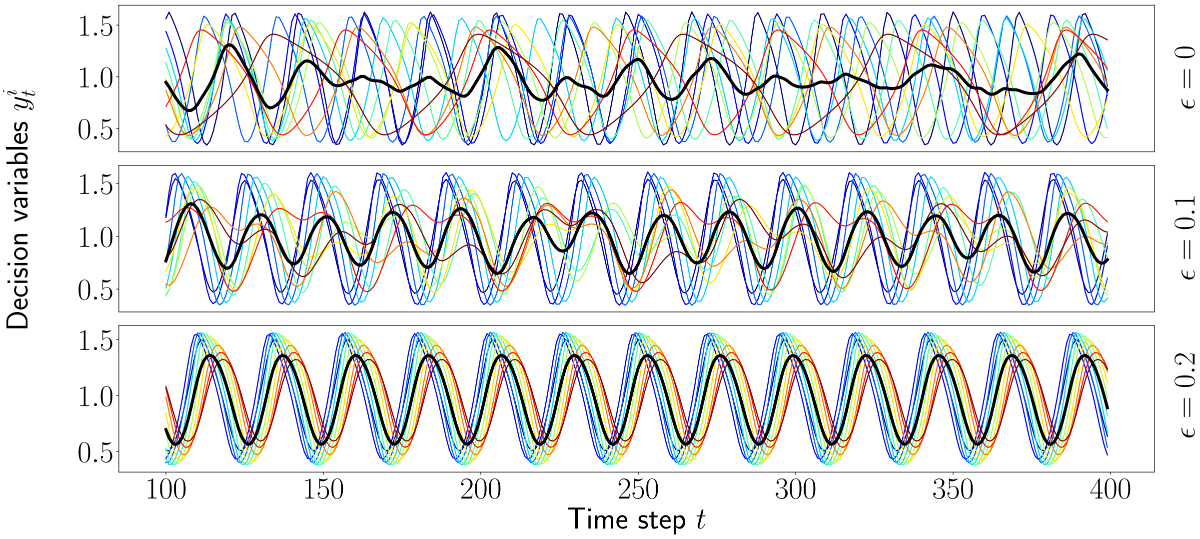

Figure 3: Time series generated by model (1) for a complete interaction network with $N = 10$ agents, for three values of the coupling coefficient ϵ. Colors from blue to red indicate time series that have higher to lower frequencies. Thick black lines are averages over the decision variables of the agents, which could be interpreted as aggregate business cycles.

the top panel, corresponding to $\epsilon = 0$, the system is uncoupled. It is possible to see that the frequencies of oscillation are heterogeneous, with periods T^i ranging from 20 time units to 66 time units. There is of course no indication of synchronization: the frequencies do not entrain, and the relative phases keep changing (there is no phase locking). Also, the shapes of the various oscillations are really different. Unsurprisingly, aggregating decision variables (thick black line) does not lead to any aggregate business cycle: aggregate fluctuations are much smaller than individual oscillations. In the middle panel, for $\epsilon = 0.1$, it is clearly possible to see that the frequencies have become similar, and some phases locked to one another. Yet, the shapes of some oscillations have remained quite different from the others, as can be seen from aggregate fluctuations still being quite smaller than individual oscillations. Finally, in the bottom panel the coupling strength is increased to $\epsilon = 0.2$. Now, not only the frequencies are the same and the phases are locked; also the shapes of oscillation have become identical, and phases are also very close across agents. The aggregate business cycle has a similar amplitude to individual oscillations. Further increasing ϵ makes individual dynamics more and more alike.

While this example was useful to build intuition, we now analyze synchronization behavior more in detail. This is done in Figure 4. Each row represents a different combination of network structure and frequency dispersion. In the first two rows, agents are connected in a complete network; in the third row, interactions occur through a star network; in the fourth row, the network is a chain. In the first, third and fourth row the values of α_1^i are evenly spaced in the interval $[-0.1, -0.02]$, leading to a frequency range $\omega^i \in [0.1, 0.3]$; in the second row, $\alpha_1^i \in [-0.4, -0.02]$, leading to $\omega^i \in [0.1, 0.8]$. This latter case corresponds to stronger frequency dispersion.

Panels in the first column represents two indicators that are commonly used to measure similarity between time series. The average correlation coefficient, typically used in the economics literature, is simply obtained by calculating the mean of all pairwise Pearson correlation coefficients between simulated time series. Phase coherence, popular in the synchronization community, measures instead similarity of phases. It is obtained by calculating the phase of each of the N oscillators at each time t, and then averaging across agents and across time. More precisely, focus on agent i. Letting t_l be the time step corresponding to the previous maximum of her decision variable y^i, and t_r be the time step of the following maximum, the phase ϕ^i at t is defined as $\phi_t^i = 2\pi(t - t_l)/(t_r - t_l)$. For example, if

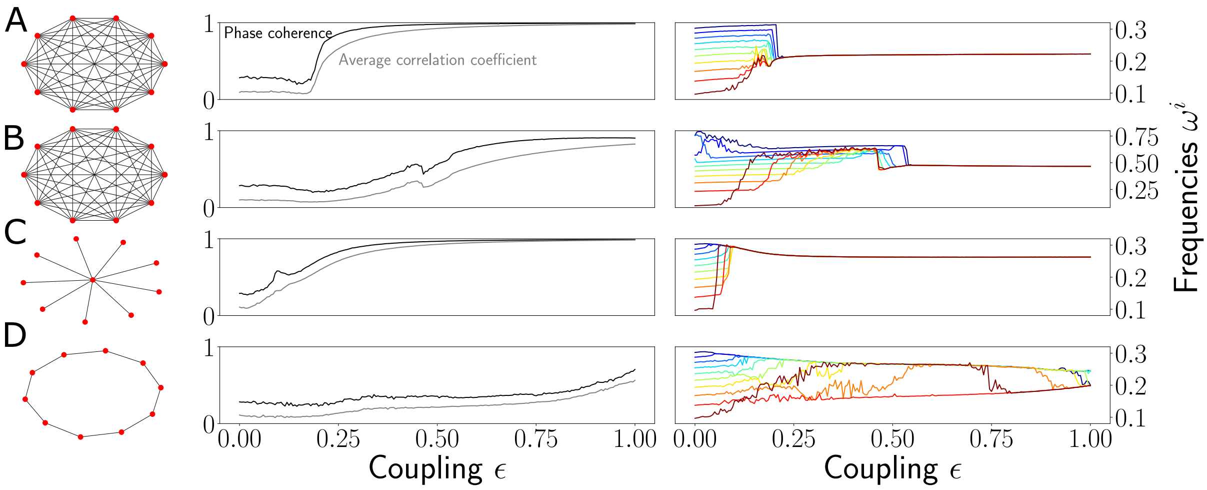

Figure 4: Phase synchronization in four cases A-D. Cases A and B are different because the frequency spread is higher in case B. Cases C and D have the same frequency spread as case A, but consider different interaction networks (star and chain, respectively). For all values of coupling $\epsilon \in [0, 1]$, we give: (i) phase coherence and average correlation coefficient; (ii) Frequencies $\omega^i = 2\pi/T^i$ of the agents. Highest (lowest) uncoupled frequencies are colored blue (red).

$t = 100$, and the closest maxima of the time series are at $t_l = 86$ and $t_r = 120$, the phase is $\phi_{t=100} = 2.58 = 2\pi \cdot 0.41$. Phase coherence at t is the modulus r_t of the complex number $r_t e^{\mathtt{I}\Phi_t} = 1/N \sum_{i=1}^{N} e^{\mathtt{I}\phi_t^i}$. ($\mathtt{I}$ in the exponential is the imaginary unit.) When all oscillators are at a similar point along the cycle (i.e. their phase is similar), r_t is close to one. If they are evenly spaced on the unit circle, r_t tends to zero. Phase coherence r is finally defined as an average over t. As we will see, the correlation coefficient and phase coherence give the same results.

Panels in the second column show how the different frequencies entrain, i.e. how they become similar to one another as the coupling strength ϵ increases. Each of the $N = 10$ lines represents the frequency of a given agent. Here and in what follows, we follow a color code that assigns blue to higher frequencies and red to lower ones.

Consider now the first row, case A. It is apparent that synchronization occurs abruptly. It is well-known in synchronization theory that this could happen, especially when the number of agents is large: it is an example of a *phase transition*. Both phase coherence and the average correlation coefficient increase abruptly at $\epsilon = 0.2$. Also the frequencies entrain at the same value of ϵ. Interestingly, the first frequency that adjusts to the others is the lowest frequency (largest periodicity), while the highest frequency is the last one to adjust. The frequency of the coupled system is close to the arithmetical average of the frequencies of the uncoupled agents.

The second row (case B) is analogous to the first row except that the parameters α_1^i are selected in the larger interval $[-0.4, -0.02]$, leading to stronger frequency dispersion. Unsurprisingly, synchronization is harder, and is obtained only for a much larger value of ϵ. As in the previous case, the first frequency that adjusts is the smallest one. Interestingly, there is little evidence for a phase transition, as the transition to synchronized behavior is smoother (but this could be due to finite size effects, given that we only have $N = 10$ agents).

In the third row (case C) agents have the same parameters as in the first row ($\alpha_1^i \in [-0.1, -0.02]$), but the interaction network is a star. This situation is the one in which synchronization occurs first. This is because all agents are connected to the central node of the star network, which acts as a "hub". Indeed, it is possible to see in the figure that when frequencies adjust, they first adjust to the frequency of the central node, as opposed to adjusting to the average frequency (cases A and B). These results are in line with known results about synchronization of "scale-free" networks (Arenas et al., 2008), which have many

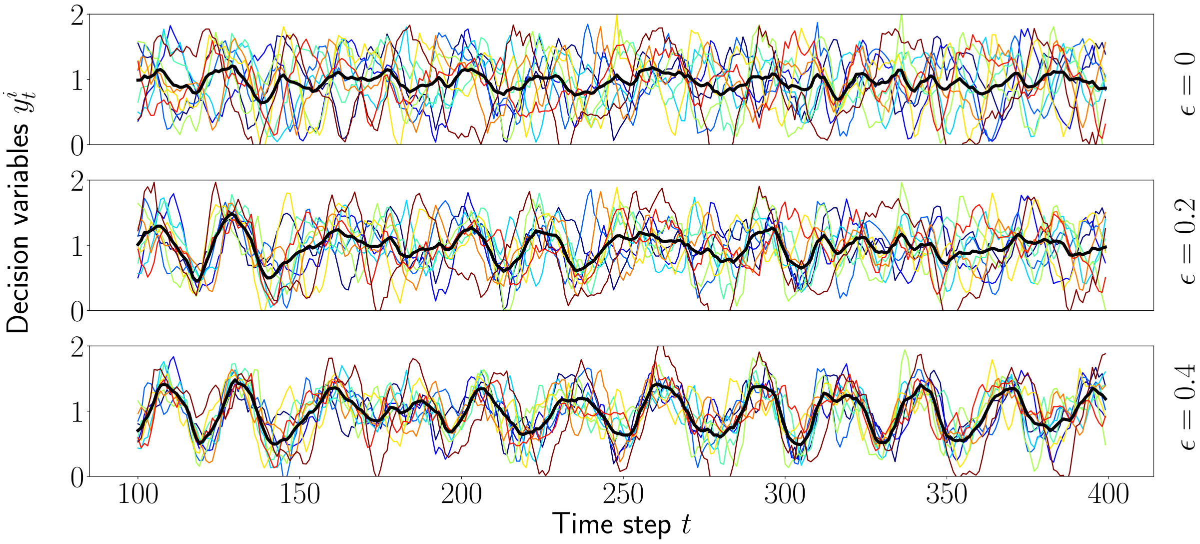

Figure 5: Time series generated by model (1) augmented by idiosyncratic noise u_t^i. As in Figure 3, we consider a complete interaction network with $N = 10$ agents, for three values of the coupling coefficient ϵ.

hubs that have a similar effect to the central node in the star network that we consider. As an arbitrary choice, we have assigned the central agent the highest frequency. Interestingly, we also find that the common frequency of oscillation—the one to which all agents converge if ϵ is high enough—is no longer the arithmetical average between the uncoupled frequencies, but is much closer to the uncoupled frequency of the central node.

Finally, the fourth row (case D) is a situation in which interactions are mediated by a chain network. This situation is the one in which synchronization is most difficult. The most likely reason is limited interactions due to local connectivity.[21]

Stochastic cycles. Two noise terms appear in Eq. (1). Idiosyncratic noise u_t^i can be expected to act as a desynchronizing force, since, by definition, it affects each agent differently. It is a priori unclear, however, to which extent phase synchronization is possible under idiosyncratic noise. Eq. (1) also contain a common noise term v_t. It is well known in synchronization theory that common noise makes frequency entrainment possible even in the absence of coupling. The synchronization literature typically deals with noise by transforming phase equations into stochastic differential equations, and showing that the main results of synchronization theory are robust to noise (Pikovsky et al., 2003). Analytical results make strong simplifying assumptions on the type of noise and coupling. Here, we address synchronizability under noise by performing numerical simulations.

Figure 5 shows example time series, under relatively strong idiosyncratic noise, parameterized as an AR(1) process with persistence $\rho_u = 0.5$ and standard deviation of the (normal) innovation term $\sigma_u = 0.1$, which is 10% of the steady-state value of the decision variables y^i. As in Figure 3, the top panel shows dynamics of isolated agents ($\epsilon = 0$). Differently from the deterministic case, idiosyncratic shocks make individual fluctuations resemble economic time series much more. Yet, similarly to the deterministic scenario, no aggregate business cycle emerges, as individual fluctuations cancel out. We then consider stronger coupling $\epsilon = 0.2$. This was more than enough to achieve synchronization in the deterministic system, but it is not enough here. We need to assume much stronger coupling, $\epsilon = 0.4$, to obtain a sufficiently strong level of synchronization. This also confirms, however, that phase synchronization is still possible under idiosyncratic shocks. Further confirmation comes from a systematic investigation that is analogue to the one in Figure 4 (results not reported here;

[21] The seminal paper on small-world networks by Watts and Strogatz (1998) was precisely conceived to enhance synchronizability of chain networks by creating "shortcuts" across the network.

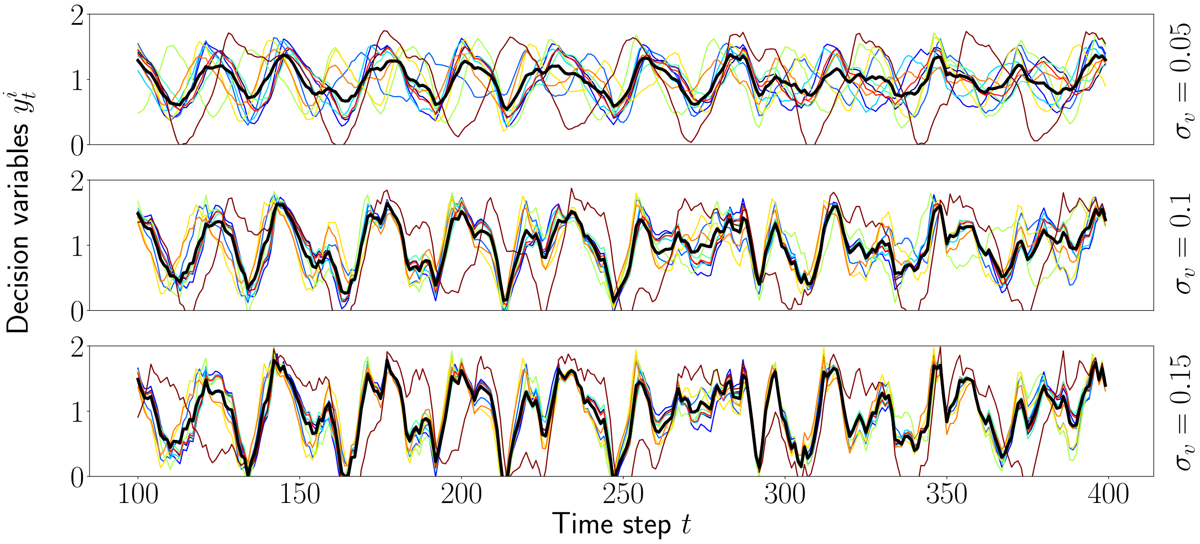

Figure 6: Time series generated by model (1) augmented by common noise v_t^i, with standard deviation σ_v. No further coupling exists: $\epsilon = 0$.

see Pangallo 2019)

We now consider common noise v_t^i. To focus on the synchronizing effect of common noise, we exclude any other coupling by setting $\epsilon = 0$. We keep the correlation of the AR(1) process fixed to $\rho_v = 0.5$, while we vary the standard deviation of the innovation term. This takes increasing values $\sigma_v = 0.05$, $\sigma_v = 0.10$ and $\sigma_v = 0.15$. In Figure 6 we show that stronger common noise leads to stronger synchronization, but also to weaker periodicity. Interestingly, while the first frequency that adjusts to the others under coupling is the lowest one (see Figure 4), under common noise the lowest frequency is the one that adjusts last. These results support common shocks (Lucas, 1977) as a possible synchronization channel, although the level of synchronization that is achieved under common noise is not as strong as under coupling.

4.2 Input-output specification

We now study phase synchronization of the input-output model described in Section 3.2 (Eq. 5). We always select parameters so that phase synchronization is achieved; our main research question is which sectors/countries have more power in determining the common frequency of oscillation. We first focus on the US input-output network in isolation, by removing all the edges pointing to other countries, which in any case account for only about 5% of the value flows. We then consider the opposite case in which we aggregate all sectors within any given countries and study the international synchronization of business cycles. In this section we only consider deterministic dynamics, as results for stochastic dynamics are similar.

Synchronization centrality in the US input-output network. Starting from the raw data,[22] we calculate the interaction coefficients w_{kj}^{ij}, for $i, k \in [0, \dots, I]$ and j corresponding to the United States. Following our discussion in Section 3.2, we obtain the interaction coefficients for sectors by dividing the value flows by the total output of each sector. We instead calculate the interaction coefficients for final demand by considering the output share of each sector. In network terms, final demand is a node with outgoing weighted edges to all other nodes, such that the weight of the edges is proportional to the total out-strength of the pointed nodes.

[22] We use the World Input-Output Database for year 2000. See Section 6 for a description of these data and for an explanation on why we choose them.

Table 1 shows the interaction matrix for 10 macro sectors and final demand. The first 10 rows in Table 1 are the shares of output that flow from the row to the column. For example, 0.58 in the first row means that 58% of "AtB - agriculture" output flows to manufacturing, and 0.18 in the same first row means that 18% of agriculture output is directly consumed ("FinD" - Final Demand). The 11-th FinD row simply shows the output shares of the various sectors. The two largest sectors are "JtK - Finance and other business services", with 28% of the output share, and "D - Manufacturing", with 21%.

Table 1: Input-Output US

Sector	AtB	C	D	E	F	GtH	I	JtK	LtN	OtP	FinD
AtB	0.22	0.0	0.58	0.0	0.0	0.01	0.0	0.0	0.01	0.0	0.18
C	0.0	0.04	0.49	0.25	0.04	0.0	0.01	0.01	0.02	0.0	0.12
D	0.01	0.01	0.35	0.0	0.06	0.05	0.03	0.03	0.07	0.01	0.39
E	0.02	0.02	0.21	0.0	0.01	0.1	0.02	0.12	0.1	0.02	0.38
F	0.0	0.0	0.01	0.01	0.0	0.01	0.01	0.05	0.04	0.0	0.87
GtH	0.0	0.0	0.1	0.0	0.04	0.04	0.01	0.05	0.04	0.01	0.7
I	0.01	0.0	0.12	0.03	0.03	0.09	0.14	0.11	0.08	0.03	0.36
JtK	0.0	0.01	0.08	0.01	0.02	0.07	0.03	0.25	0.08	0.03	0.42
LtN	0.0	0.0	0.01	0.0	0.0	0.01	0.0	0.01	0.02	0.0	0.95
OtP	0.0	0.0	0.05	0.0	0.02	0.04	0.05	0.11	0.07	0.09	0.58
FinD	0.01	0.01	0.21	0.02	0.06	0.14	0.06	0.28	0.16	0.04	0.0
EigC	0.01	0.01	0.18	0.01	0.04	0.08	0.04	0.16	0.10	0.03	0.35
SyncCL	0.01	0.01	0.18	0.01	0.04	0.07	0.04	0.17	0.10	0.03	0.36
SyncCH	0.01	0.00	0.17	0.01	0.04	0.07	0.04	0.16	0.09	0.02	0.39

Note: AtB: Agriculture; C: Mining; D: Manufacturing; E: Utilities; F: Construction; GtH: Trade; I: Transports; JtK: Finance and other business services; LtN: Government services; OtP: Other services; FinD: Final demand.

From this table, it is not obvious which sectors have a strongest influence on determining the common frequency of oscillation, in case phase synchronization is obtained. One could argue that the size of sectors (i.e., their share of output) should be directly proportional to this importance. For example, it could be that "JtK - Finance and other business services" is more important than "D - Manufacturing" in determining the frequency of oscillations, because the business sector is larger than the manufacturing sector. However, some sectors are more central in the network of intermediate goods, while other sectors depend more strongly on final demand, so that network position could also be an important determinant.

As a first pass to take these feedback effects into account, we calculate the Eigenvector Centrality of the weighted network represented in Table 1, with $N + 1 = 11$ nodes. This input-output table is a row-stochastic matrix with all positive entries, so the first left eigenvector of the matrix gives the Eigenvector Centrality. This also corresponds to the steady state of a Markov Chain defined on this matrix. The results are reported in the line "EigC" in Table 1. The most interesting result is that "D - Manufacturing" is more important than "JtK - Business" in terms of this centrality measure, precisely because the higher requirement of intermediate inputs in manufacturing makes many sectors of the economy depend on manufacturing demand.

We now perform simulations to explicitly see which sectors are most important in determining the frequency of oscillations. As in the previous section, we obtain heterogeneous frequencies by assigning different values of the accumulation dislike parameter α_1^i, $\alpha_1^i \in [-0.1, -0.02]$, to different nodes. We implement the following algorithm.

1. We focus on a sector, say "AtB - Agriculture", and we assign it the lowest (L) frequency of oscillation (i.e. $\alpha_1^i = -0.02$).

2. For 1000 times, we randomly assign the other frequencies of oscillation to the remaining sectors.
3. For each of these 1000 times, we simulate the model in Eqs. (5), calibrated on the US input-output network, and calculate the common frequency of oscillation (under the frequency spread that we consider and the interaction network based on the US input-output network, phase synchronization is always obtained).
4. We repeat the three steps above focusing on each of the 11 nodes in turn.
5. For each focus sector, we average the common oscillation frequencies across random assignments. We end up with a vector of 11 averaged frequencies obtained by assigning the lowest frequency to any focus sector and averaging across many possible assignments of the other frequencies to the other sectors.
6. We compare these 11 averaged frequencies to a benchmark frequency obtained by simulating the model on a uniform weight matrix, that is a matrix in which all entries are $1/(N+1)$. If any averaged frequency is smaller than the benchmark frequency, it means that the focus sector is more important in setting the common frequency of oscillation than in the uniform benchmark case. If the frequency is larger, it means that it is less important.
7. By taking the difference between the benchmark frequency and each of the 11 averaged frequencies, we obtain positive and negative numbers. We add the absolute value of the minimum number to make all averaged frequencies non-negative, and we normalize them so that they sum to unity. The resulting *synchronization centrality* measure, that we denote *SyncCL* (L stands for "Lowest frequency assigned to the focus sector"), is reported in the second-to-last row in Table 1.
8. We repeat the above procedure assigning the highest (H) frequency to the focus sector. The corresponding synchronization centrality measure, that we denote *SyncCH*, is reported in the last row in Table 1.

As is possible to see, both synchronization centrality measures are strongly correlated to eigenvector centrality. Therefore these simulations support the fact that eigenvector centrality could be taken as a measure of the importance of each node in determining the common frequency of oscillation. This confirms the finding that manufacturing has more power than business services in setting the common frequency, because it is more central in the intermediate good flows of the economy.

A final important point is about the robustness of these results to disaggregation. For example, if, instead of considering an aggregate manufacturing sector, we had considered 11 manufacturing sub-sectors, would we get the same results by ex-post aggregating the sub-sectors? In other words, when is it legitimate to aggregate sub-sectors into macro-sectors and when is it not? Ultimately, when is it legitimate to aggregate individual firms into sectors?

One possible answer was already given in Section 4.1. If firms in a given sector, or if sub-sectors that are part of a macro-sector, are hit by common shocks, this synchronizes their frequencies. So one could consider the subsector or the macro-sector directly as the relevant unit of synchronization. However, such explanation is only partly satisfactorily, especially given that, as shown in Figure 6, synchronization through common noise is not really strong.

To address this issue, we compare the eigenvector centrality for the 10 macro-sectors (plus final demand) in Table 1 to the eigenvector centrality calculated from an equivalent weight matrix with 27 sectors (and final demand). These sectors comprise manufacturing and service subsectors and the smallest sectors in Table 1, such as "AtB - Agriculture", "C - Mining" and "E - Utilities". The eigenvector centrality is a vector with 28 elements. Aggregating these back into the 11 elements in Table 1, we get that the vector of centrality measures is identical to the one in Table 1 up to two significant digits.

This example suggests that the importance of nodes in determining the common frequency of oscillation is independent of the level of aggregation, to the extent that synchronization centrality always corresponds to eigenvector centrality.

Synchronization of international business cycles. We now aggregate all sectors within a country, including final demand, and study the international synchronization of endogenous business cycles. We only focus on 17 advanced economies which had a fairly similar development in the last 60 years. These are the US, Canada, Australia, Japan, and 13 European countries (UK, France, Germany, Italy, Portugal, Spain, Belgium, Austria, Ireland, Netherlands, Denmark, Sweden, Finland).

Table 2: International Input-Output (Year 2000)

Country	AUS	AUT	BEL	CAN	DEU	DNK	ESP	FIN	FRA	GBR	IRL	ITA	JPN	NLD	PRT	SWE	USA
AUS	0.93	0.0	0.0	0.0	0.0	0.0	0.0	0.0	0.0	0.01	0.0	0.0	0.03	0.0	0.0	0.0	0.02
AUT	0.0	0.64	0.01	0.0	0.17	0.0	0.01	0.0	0.02	0.03	0.0	0.05	0.01	0.01	0.0	0.01	0.03
BEL	0.0	0.01	0.57	0.0	0.1	0.01	0.02	0.0	0.09	0.05	0.0	0.04	0.01	0.05	0.0	0.01	0.04
CAN	0.0	0.0	0.0	0.66	0.01	0.0	0.0	0.0	0.0	0.01	0.0	0.0	0.01	0.0	0.0	0.0	0.29
DEU	0.0	0.01	0.02	0.0	0.8	0.0	0.01	0.0	0.04	0.02	0.0	0.02	0.01	0.01	0.0	0.01	0.03
DNK	0.0	0.0	0.01	0.0	0.06	0.7	0.01	0.01	0.02	0.03	0.01	0.01	0.01	0.01	0.0	0.06	0.04
ESP	0.0	0.0	0.01	0.0	0.03	0.0	0.85	0.0	0.04	0.01	0.0	0.02	0.0	0.01	0.02	0.0	0.01
FIN	0.0	0.01	0.01	0.01	0.07	0.01	0.02	0.67	0.03	0.05	0.0	0.02	0.01	0.02	0.0	0.04	0.03
FRA	0.0	0.0	0.02	0.0	0.04	0.0	0.02	0.0	0.83	0.02	0.0	0.02	0.0	0.01	0.0	0.0	0.02
GBR	0.0	0.0	0.01	0.01	0.04	0.0	0.01	0.0	0.02	0.82	0.02	0.01	0.01	0.01	0.0	0.01	0.04
IRL	0.0	0.0	0.02	0.01	0.08	0.0	0.01	0.0	0.04	0.09	0.49	0.02	0.02	0.01	0.0	0.01	0.18
ITA	0.0	0.0	0.01	0.0	0.03	0.0	0.01	0.0	0.03	0.01	0.0	0.87	0.0	0.0	0.0	0.0	0.02
JPN	0.0	0.0	0.0	0.0	0.0	0.0	0.0	0.0	0.0	0.0	0.0	0.0	0.96	0.0	0.0	0.0	0.02
NLD	0.0	0.01	0.06	0.0	0.09	0.01	0.01	0.0	0.04	0.05	0.01	0.03	0.01	0.62	0.0	0.01	0.04
PRT	0.0	0.0	0.01	0.0	0.03	0.0	0.04	0.0	0.02	0.02	0.0	0.01	0.0	0.01	0.83	0.0	0.01
SWE	0.0	0.01	0.02	0.01	0.06	0.04	0.01	0.02	0.02	0.04	0.0	0.02	0.01	0.02	0.0	0.7	0.04
USA	0.0	0.0	0.0	0.02	0.0	0.0	0.0	0.0	0.0	0.0	0.0	0.0	0.01	0.0	0.0	0.0	0.95
Output	0.02	0.01	0.01	0.03	0.08	0.01	0.03	0.01	0.06	0.06	0.00	0.05	0.20	0.02	0.00	0.01	0.42
EigC	0.01	0.01	0.01	0.03	0.08	0.01	0.04	0.00	0.07	0.06	0.00	0.06	0.13	0.01	0.01	0.01	0.47

Note: AUS: Australia; AUT: Austria; BEL: Belgium; CAN: Canada; DEU: Germany; DNK: Denmark; ESP: Spain; FIN: Finland; FRA: France; GBR: United Kingdom; IRL: Ireland; ITA: Italy; JPN: Japan; NLD: Netherlands; PRT: Portugal; SWE: Sweden; USA: United States

To start, we consider the equivalent version of Table 1 in which, instead of having sectors and final demand, we only have countries. In Table 2, each row-column pair indicates the flow of goods and services from row to column. For example, 0.03 at the “AUS” row and “JPN” column indicates that 3% of the Australian output is sold to Japan. The diagonal of this matrix is the fraction of the value flows that stays within a country, in the same way as the diagonal of Table 1 was indicating the fraction of value flows that was staying within a sector.

The difference is immediate. While most of what was produced within a sector was flowing to other sectors, most of what is produced within a country stays within the same country. This ranges from 96% in the case of Japan and 95% in the case of the US, to 49% in the case of Ireland. On average, 90% of the value flows stay within the same country.[23]

In Table 2, the Eigenvector Centrality is strongly correlated to the shares of output. The US have Eigenvector Centrality 0.47, while the European countries, combined, have 0.35. This shows that, according to the model and the used data, the US have most power in setting the rhythms of global business cycles, and precisely quantifies this power.

[23]While these data refer to year 2000, when globalization had not completely taken off yet, Cerina et al. (2015) show that the foreign share of value flows had only increased to about 12.5% in 2011, after a small dip corresponding to the 2008 financial crisis. Likewise, the foreign share in year 1995 was only 1% smaller than in year 2000.

5 Complete synchronization

All analysis of phase synchronization so far was concerned with the conditions under which the frequencies of oscillation of different agents could become similar. This analysis is limited by the extent to which we can empirically measure the uncoupled frequency of a sector or a country. It is also limited by the assumption that endogenous business cycles can be described by non-linear dynamic models that exhibit relatively clear periodicity. One may want to consider a chaotic business cycle model that produces irregular time series, and phase synchronization would be of little use. In this section, we study synchronization from a different perspective. We assume that the frequencies of oscillation are identical, and we explore the conditions under which complete synchronization can emerge, i.e. the non-linear dynamics of the agents become perfectly aligned. Since we are studying a limit cycle model, complete synchronization is always obtained absent shocks. Yet, the theory of complete synchronization that we develop can be used to study the interplay between synchronizing non-linear dynamics, exogenous shocks and network structure. It does so by exploring how shocks propagate on the interaction network on the path back to synchronization.

As we did in Section 4, we first study complete synchronization in an abstract interaction network (Section 5.1), and then we consider input-output networks (Section 5.2).

5.1 Abstract interaction network

To study the interplay between synchronizing dynamics, shock propagation and network structure, we adapt the master stability approach originally proposed by Pecora and Carroll (1998). We start by assuming that all agents are in a synchronized state $\boldsymbol{s}_t = (x^s_t, y^s_t)$ in which they all behave alike, i.e. $x^i_t = x^s_t$ and $y^i_t = y^s_t$, $\forall i$. This synchronized state could have been reached after an initial transient. The starting point of the master stability approach is to calculate the relative strength of desynchronizing forces that lead to deviations from the synchronized state, and synchronizing forces due to coupling. Here, desynchronizing forces only correspond to idiosyncratic shocks u^i_t, because limit cycles are attractive. However, in the case of chaotic dynamical systems, chaos acts as a desynchronizing force, too. The key idea of the master stability approach is to perform a transformation that uncouples the deviations from the synchronized state into orthogonal components. The approach is semi-analytical, in the sense that the relative strength of synchronizing and desynchronizing forces is obtained by numerically computing Lyapunov exponents, but once these are computed, the key insights are obtained analytically.

In the following, we first derive our key equations, and then provide some examples that clarify the working of our approach.

5.1.1 Theory of complete synchronization

Let $x^i_t = x^s_t + x^{\xi,i}_t$ and $y^i_t = y^s_t + y^{\xi,i}_t$. Here, $x^{\xi,i}_t$ and $y^{\xi,i}_t$ denote a small deviation from the synchronized state, for example due to idiosyncratic noise hitting sector i. Let further $\boldsymbol{\xi}_t = \left(x^{\xi,1}_t, y^{\xi,1}_t, x^{\xi,2}_t, y^{\xi,2}_t, \dots x^{\xi,N}_t, y^{\xi,N}_t\right)$ be the $2N$-dimensional vector of deviations.

To show how the evolution of this vector can be obtained, we fully work out a specific example. Consider a star network with three nodes. This is composed by a central node, which we denote as node 1, that is linked to two leaf nodes, which we denote as nodes 2 and 3. The leaf nodes are only connected to the central node. Replacing $x^i_t = x^s_t + x^{\xi,i}_t$ and $y^i_t = y^s_t + y^{\xi,i}_t$ in Eq. (1) and assuming, as we did in Section 4.1, that the dependence on other nodes is ϵ/k_i, where k_i is degree of node i, while the dependency on oneself is $1 - \epsilon$, we get the following system of equations for the evolution of $\boldsymbol{\xi}_t$:

$$\begin{cases} x_{t+1}^{\xi,1} = (1-\delta)x_t^{\xi,1} + y_t^{\xi,1}, \\ y_{t+1}^{\xi,1} = \alpha_1 x_t^{\xi,1} + (\alpha_2 + F'(y_t^s))\, y_t^{\xi,1} - \epsilon F'(y_t^s)\left(y_t^{\xi,1} - \frac{1}{2}y_t^{\xi,2} - \frac{1}{2}y_t^{\xi,3}\right), \\ x_{t+1}^{\xi,2} = (1-\delta)x_t^{\xi,2} + y_t^{\xi,2}, \\ y_{t+1}^{\xi,2} = \alpha_1 x_t^{\xi,2} + (\alpha_2 + F'(y_t^s))\, y_t^{\xi,2} - \epsilon F'(y_t^s)\left(y_t^{\xi,2} - y_t^{\xi,1}\right), \\ x_{t+1}^{\xi,3} = (1-\delta)x_t^{\xi,1} + y_t^{\xi,1}, \\ y_{t+1}^{\xi,3} = \alpha_1 x_t^{\xi,1} + (\alpha_2 + F'(y_t^s))\, y_t^{\xi,1} - \epsilon F'(y_t^s)\left(y_t^{\xi,3} - y_t^{\xi,1}\right), \end{cases} \tag{12}$$

where we have used the fact that the deviations $\boldsymbol{\xi}_t$ are small, to Taylor-expand the function F to first order. This formulation suggests that the evolution of deviations of any single node is given by the Jacobian of the dynamics corresponding to that node, plus a term of interaction with other nodes. Extrapolating from this example, it is easy to see that the evolution of the whole vector $\boldsymbol{\xi}_t$ is generally given by

$$\boldsymbol{\xi}_{t+1} = (\boldsymbol{I}_N \otimes \boldsymbol{J}(\boldsymbol{s}_t) - \epsilon F'(\boldsymbol{s}_t)\boldsymbol{KLK} \otimes \boldsymbol{H})\, \boldsymbol{\xi}_t, \tag{13}$$

where

- $\boldsymbol{I}_N$ is the N-dimensional identity matrix.
- $\boldsymbol{J}(\boldsymbol{s}_t)$ is the 2-dimensional Jacobian.
- $\otimes$ denotes the Kronecker product, i.e. a $2N$-dimensional matrix.
- $F'(\boldsymbol{s}_t)$ is the first derivative of F, due to the fact that we are considering a first-order approximation around the synchronized state.
- $\boldsymbol{K}$ is an N-dimensional square matrix with $1/\sqrt{k_i}$ on the main diagonal and zero everywhere else.
- $\boldsymbol{L}$ is the Laplacian of the network. This is a key mathematical property of the network that is widely used in many applications. $L_{ii} = k_i$ and $L_{ij} = -1$ if i and j are connected. $\boldsymbol{KLK}$ is known as normalized Laplacian, and has similar properties to the Laplacian.[24]
- $\boldsymbol{H}$ is the 2-dimensional square matrix of connectivity in the dynamical system. Since here the only connectivity is through y, it is $H_{22} = 1$ and zero everywhere else.

The problem with Eq. (13) is that the evolution of each component $y_t^{\xi,i}$ depends on all other agents j to which i is connected. The key trick of the master stability approach is to diagonalize $\boldsymbol{KLK}$ so to decompose the deviations $\boldsymbol{\xi}$ into orthogonal, uncoupled, components. Following the terminology in the literature, we call these components *eigenmodes*. Let $\boldsymbol{\xi}_t = (\boldsymbol{Q} \otimes \boldsymbol{I}_2)\, \boldsymbol{\zeta}_t$, where Q is the matrix of eigenvectors of $\boldsymbol{KLK}$. Here, $\boldsymbol{\zeta}_t$ can be interpreted as a projection of $\boldsymbol{\xi}_t$ in the eigenspace. It evolves according to

$$\boldsymbol{\zeta}_{t+1} = (\boldsymbol{I}_N \otimes \boldsymbol{J}(\boldsymbol{s}_t) - \epsilon F'(\boldsymbol{s}_t)\boldsymbol{\Lambda} \otimes \boldsymbol{H})\, \boldsymbol{\zeta}_t, \tag{14}$$

where $\boldsymbol{\Lambda}$ is the matrix with the eigenvalues of $\boldsymbol{KLK}$ on the main diagonal and zero everywhere else. Each of the N eigenmodes of $\boldsymbol{\zeta}_t$ can then be written as

$$\zeta_{t+1}^i = (\boldsymbol{J}(\boldsymbol{s}_t) - F'(\boldsymbol{s}_t)\epsilon\lambda_i \boldsymbol{H})\, \zeta_t^i. \tag{15}$$

[24] Here we summarize a few properties of $\boldsymbol{KLK}$. Because the rows sum to zero, one eigenvalue is zero. Moreover, it is well known that the other eigenvalues are positive and bounded between 0 and 2. The multiplicity of the 0 eigenvalue reflects the number of disconnected clusters in the network. We sort the eigenvalues in increasing order, so that $\lambda_1 = 0$, $\lambda_2 > 0$ if the network is connected, $\lambda_3 \geq \lambda_2$, ..., $\lambda_N \geq \lambda_{N-1}$, $\lambda_N \leq 2$. The eigenvalue λ_2 is knows as *algebraic connectivity* and the corresponding eigenvector as *Fiedler vector*. The smaller λ_2, the more the network has a modular structure, in which two or more clusters of nodes have strong internal connectivity and weak external connectivity. In the case of two clusters, the components of the Fiedler vector are positive for nodes in a cluster and negative for nodes in the other cluster. Fiedler vectors are commonly used for graph partitioning.

In this basis, the evolution of each eigenmode i only depends upon itself. We stress that i now is an eigenvector (corresponding to the eigenvalue λ_i of the normalized Laplacian of the network) and *not to an agent*. As will be clear in the examples below, the evolution of each eigenmode corresponds to higher-order properties of the network. Of course one can retrieve the dynamics of the agents by applying the transformation $\boldsymbol{\xi}_t = (\boldsymbol{Q} \otimes \boldsymbol{I}_2)\,\boldsymbol{\zeta}_t$.

The eigenmode $i = 1$, corresponds to dynamics parallel to the synchronization manifold (i.e., "in the same direction as the dynamics"). It captures the phase shift due to a shock hitting the system at a given time t, as will be clarified below. The eigenmodes $i > 1$ correspond to dynamics orthogonal to the synchronization manifold. If these dynamics always converge to zero after the shock, the synchronized state is stable.

Whether the orthogonal dynamics converge to zero is not obvious from Eq. (15). To know if they do, one must numerically compute the Lyapunov exponents of the system. Letting $K = \epsilon\lambda_i$ denote an effective coupling for eigenmode i, one calculates Lyapunov exponents in Eq. (15) for all values of K that are typically obtained. In our case, because $\epsilon \in [0, 1]$ and $\lambda_i \in [0, 2]$, it is of interest to only consider the interval $K \in [0, 2]$.

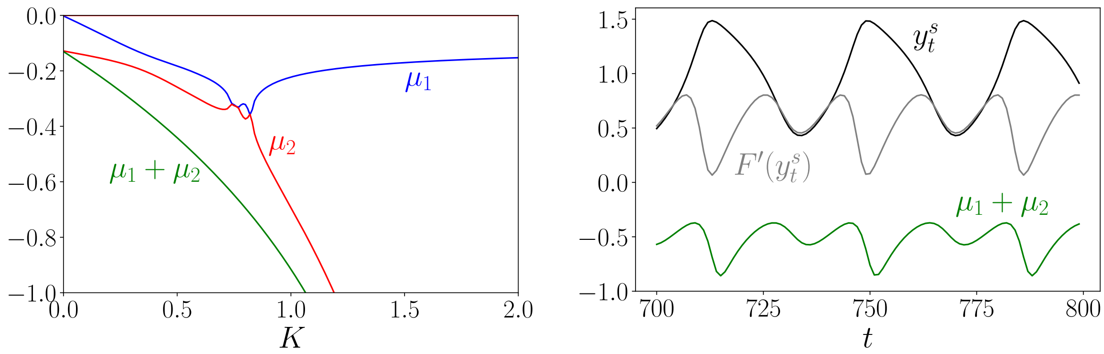

(a)

(b)

Figure 7: (Left) Time-averaged Lyapunov exponents μ_1 and μ_2, and sum $\mu_1 + \mu_2$, as a function of the effective coupling K. (Right) Time evolution of the sum of Lyapunov exponents $\mu_1 + \mu_2$, compared to the time evolution of y at the synchronized state y_t^s, and to the time evolution of $F'(y_t^s)$.

The Lyapunov exponents are shown in Figure 7, for a parameterization of the model that we will specify in the examples below, Section 5.1.2. In Figure 7a we only consider the time average of the Lyapunov exponents. The dependence of the first Lyapunov exponent μ_1 on the effective coupling K is called *master stability function*. The first thing that stands out is that both μ_1 and μ_2 are always negative. This means that perturbations along the orthogonal eigenmodes indeed vanish over time. If the system was chaotic, this would no longer be true, and the synchronized state would only be stable for certain values of K. Moreover, the largest Lyapunov exponent μ_1 is null for $K = 0$: this means that perturbations in the direction parallel to the synchronization manifold do not vanish, so that a permanent phase shift occurs. Finally, the highest values of μ_1 and μ_2 are obtained for smallest K. All else equal, it means that eigenmodes corresponding to the smallest eigenvalues λ_i are the ones that decay most slowly, while eigenmodes corresponding to relatively large eigenvalues decay much more rapidly.

As in all dynamical systems, the Lyapunov exponents are never constant, but rather vary along the attractor. Figure 7b shows the time evolution of the sum of Lyapunov exponents $\mu_1 + \mu_2$, representing the rate of expansion or contraction of volumes in phase space. The times at which $\mu_1 + \mu_2$ is minimal (most negative) are those at which the effects of shocks are weakest and most rapidly absorbed, while maximal (least negative) $\mu_1 + \mu_2$ indicates that shocks have a stronger and more lasting effect. To understand to which phases of the evolution of the system these correspond, we plot the dynamics of the synchronized state y_t^s and the time evolution of $F'(y_t^s)$. It is interesting to note that the evolution of $\mu_1 + \mu_2$ closely mirrors that of $F'(y_t^s)$. The most stable situation is when y_t^s is in a peak, followed by y_t^s being in a trough. The most unstable situations correspond instead to periods of rapid growth or recession. In these situations, shocks propagate most strongly and lead to strongest desynchronization.

In summary, our theory calculates the deviations from a synchronized state in which all agents behave alike—deviations that could for example be due to an exogenous shock hitting one agent only. This is an approximation due to the fact that we assume that deviations are small to consider a Taylor expansion of the function F. Instead of calculating the evolution of the deviations for each agent, we calculate the evolution of deviations for each eigenmode, corresponding to an eigenvector of a matrix of connectivity. This allows (i) to show that the synchronized state is stable to small shocks, but it is generally affected by a permanent phase shift; (ii) to understand how the propagation of the shock is affected by the interaction network; (iii) to understand how the propagation of the shock is affected by the timing of the shock with respect to the endogenous dynamics. Ultimately, this theory is useful to assess which level of correlation we can expect between economic time series that are modeled by our system. To get more intuition into this formalism, we now consider a number of examples.

5.1.2 Examples of complete synchronization

All parameters in the examples below are chosen following the guidelines in Section 3.3. The values of β_0, β_1, β_2, β_3, β_4, δ and α_0 are chosen as in Section 3.3. We further choose $\alpha_2 = 0.4$ and $\alpha_1 = -0.04$, which leads to a cycle of about 36 time units. If one time unit corresponds to a quarter, this cycle would have length 9 years, which is in line with the empirical evidence of employment variables in the United States (Beaudry et al., 2020). Throughout this section, for clarity we study the effect of single idiosyncratic shocks hitting the agents in the network at a certain time τ, and study its propagation. In Section 6, we will let shocks continuously hit agents, as can be expected in the real world.

Two connected agents. We start from the simplest possible system to study the interplay between dynamics and shocks in most detail. We will then consider a more interesting interaction structure to understand shock propagation. Here, we consider two connected agents, giving weight $1-\epsilon$ to their own dynamics and ϵ to dynamics of the other node. We assume $\epsilon = 0.3$. The eigenvalues of $\boldsymbol{KLK}$ are $\lambda_1 = 0$ and $\lambda_2 = 2$, the corresponding eigenvectors are $\boldsymbol{v}_1 = (1,1)/\sqrt{2}$ and $\boldsymbol{v}_2 = (-1,1)/\sqrt{2}$. After the shock hits at time τ, at time $t \geq \tau$ the deviations from the synchronized state in the initial basis and in the eigenbasis are related by the following equations:

$$\begin{aligned}
x_t^{\xi,1} &= \tfrac{1}{\sqrt{2}}\left(x_t^{\zeta,1} - x_t^{\zeta,2}\right), & x_t^{\zeta,1} &= \tfrac{1}{\sqrt{2}}\left(x_t^{\xi,1} + x_t^{\xi,2}\right), \\
y_t^{\xi,1} &= \tfrac{1}{\sqrt{2}}\left(y_t^{\zeta,1} - y_t^{\zeta,2}\right), & y_t^{\zeta,1} &= \tfrac{1}{\sqrt{2}}\left(y_t^{\xi,1} + y_t^{\xi,2}\right), \\
x_t^{\xi,2} &= \tfrac{1}{\sqrt{2}}\left(x_t^{\zeta,1} + x_t^{\zeta,2}\right), & x_t^{\zeta,2} &= \tfrac{1}{\sqrt{2}}\left(-x_t^{\xi,1} + x_t^{\xi,2}\right), \\
y_t^{\xi,2} &= \tfrac{1}{\sqrt{2}}\left(y_t^{\zeta,1} + y_t^{\zeta,2}\right), & y_t^{\zeta,2} &= \tfrac{1}{\sqrt{2}}\left(-y_t^{\xi,1} + y_t^{\xi,2}\right).
\end{aligned} \tag{16}$$

The first column of Eq. (16) already highlights an interesting pattern. Given our previous discussion in Section 5.1.1, the second eigenmode $\left(x_t^{\zeta,2}, y_t^{\zeta,2}\right)$ eventually converges to zero, because the effective coupling is $K = \epsilon\lambda_2 = 0.6 > 0$. The larger the coupling coefficient ϵ, the faster the second eigenmode converges to zero. Independently of speed, eventually both $\left(x_t^{\xi,1}, y_t^{\xi,1}\right)$ and $\left(x_t^{\xi,2}, y_t^{\xi,2}\right)$ converge to the first eigenmode $\left(x_t^{\zeta,1}, y_t^{\zeta,1}\right)$. This shows analytically that, after some time, the deviations of the two agents coincide with the perturbation parallel to the synchronization manifold, reinstating a synchronized state that is different from the initial synchronized state by a constant phase shift. This is true for every interaction structure, as the eigenvector corresponding to $\lambda_1 = 0$ is always of the type $\boldsymbol{v}_1 = (1,\ldots,1)/\sqrt{N}$, and the eigenmodes corresponding to the other eigenvalues eventually vanish.

To proceed, we assume that the single shock at time τ only hits the variables y, i.e. $y_\tau^{\xi,1} = u_1$, $y_\tau^{\xi,2} = u_2$ and $x_\tau^{\xi,1} = x_\tau^{\xi,2} = 0$. From the second column of (16) we can see that if $u_1 = u_2$, $y_{\tau+1}^{\zeta,2} = 0$, and so for all following times t, $y_t^{\zeta,2} = 0$: The eigenmode transverse to the synchronization manifold never takes positive values. In other words, because the shock is common, it does not cause any relative difference in phase between the two agents. On the contrary, $y_{\tau+1}^{\zeta,1} = \sqrt{2}u_1$ is maximal: the effect of the shock is to only shift the phase, by the maximum amount. If $u_1 > 0$, the phase is shifted forward; if $u_1 < 0$, it is shifted backwards. Consider now the reverse case $u_1 = -u_2$. Now $y_{\tau+1}^{\zeta,1} = 0$ and $y_{\tau+1}^{\zeta,2} = \sqrt{2}u_1$. In this case the transverse eigenmode is maximal, while the parallel eigenmode is null. After a transient in which the phases are different, they synchronize again, with no consequence of the shock in terms of permanent phase shift (this is the only case which does not imply a permanent phase shift).

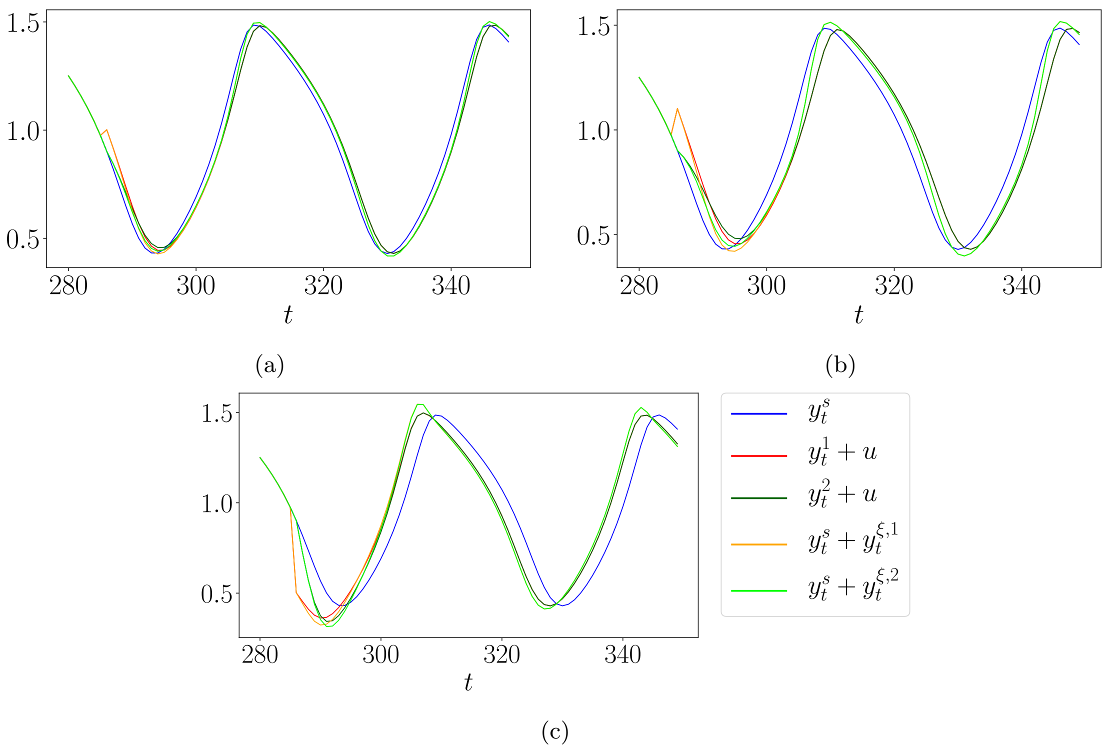

Figure 8: Effect of a shock hitting agent 1 only. Blue lines corresponds to y_t^s, the (unperturbed) synchronized state. Red and dark green lines correspond to the actual perturbed dynamics, which we denote as $y_t^1 + u$ and $y_t^2 + u$ respectively, fully simulated from dynamical system (1). The orange and light green lines correspond to the approximation of the perturbed dynamics, as obtained by Eq. (13). In panel (a), $u = 0.1$; in panel (b), $u = 0.2$; in panel (c), $u = -0.4$.

We now show some numerical simulations considering the case in which a shock hits one agent only. Without loss of generality, we set $u_1 = u$ and $u_2 = 0$. In Figure 8, we show some simulations of the dynamics, for three values of the shock u: $u = 0.1$ (Fig. 8a); $u = 0.2$ (Fig. 8b); $u = -0.4$ (Fig. 8c).

Two patterns are worth noting in Figure 8. The first is how good an approximation $y_t^s + y_t^{\xi,i}$ is to $y_t^i + u$ (the actual perturbed dynamics). The approximation is excellent for $u = 0.1$ and $u = -0.4$, but it is not as good in the case of $u = 0.2$. Note that these shocks are up to 40% of the steady state value, so the assumption of small shocks that we needed to Taylor expand the function $F(\cdot)$ definitely does not hold. Nonetheless, the approximation is still quite good. Moreover, across all cases the approximation is better at certain times. In particular, it tends to be worse in any final part of booms and recessions. As shown in Figure 7b, these correspond to times when $F'(y_t^s)$ changes rapidly, suggesting that at those times one should also consider second order terms $F''(y_t^s)$. The reason why the approximation is better for $u = -0.4$ than for $u = 0.2$, despite the first shock being twice as large in absolute value than the second one, is also due to the change in $F'(y_t^s)$. Indeed, a positive shock hitting during a recession changes the properties of the dynamics much more than a negative shock does, leading to a worse approximation. A negative shock hitting during a boom has the same effect as a positive shock hitting during a recession.

The other pattern that is worth noting in Figure 8 is the fact that a negative shock makes perturbed dynamics lag with respect to unperturbed ones, while positive shocks have the opposite effect. This result was already expected given the discussion in Section 5.1.1, but Figure 8 gives a numerical confirmation.

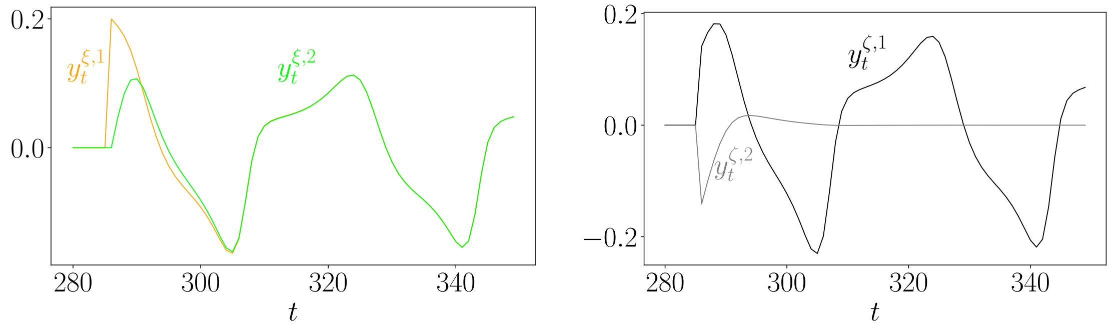

(a) (b)

Figure 9: Deviations from the synchronized state when a positive shock $u = 0.2$ hits agent 1 only. Panel (a) shows the deviations in the original basis, while panel (b) shows deviations in the eigenbasis.

In Figure 9 we show the evolution of deviations from the synchronized state in the case of $u = 0.2$. In Figure 9a, we show deviations in the original basis, $y^{\xi,1}$ and $y^{\xi,2}$. As agent 2 did not receive any shock, its dynamics slowly adjusts to that of agent 1, and after a short transient both agents get synchronized again. Figure 9b shows deviations in the eigenbasis. (Note that, because of normalization of the eigenvectors, the value of the initial shock in this basis is $0.2/\sqrt{2}$.) It is clear that the deviation orthogonal to the synchronization manifold (grey line) quickly vanishes, and only the deviation parallel to the synchronization manifold (black line) persists. This latter perturbation is the permanent phase shift.

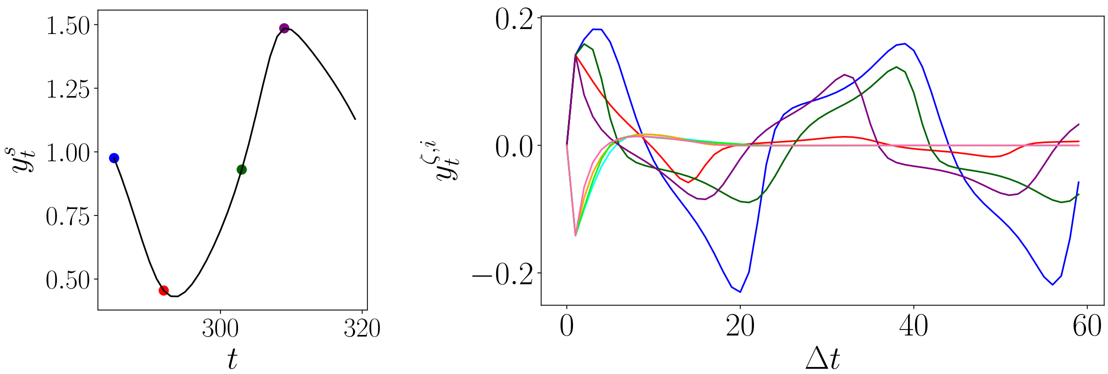

(a) (b)

Figure 10: Effect of the timing of shocks. Panel (b) shows deviations in the eigenbasis for four times at which the shock could hit: a recession (blue and cyan); a trough (red and orange); a growth period (dark and light green); a peak (purple and pink).

Finally, in Figure 10 we investigate the effect of the timing of shocks. The blue and cyan lines correspond to the same shock $u = 0.2$ at time $t = 285$, for the perturbations parallel and perpendicular to the synchronization manifold respectively. The same is true

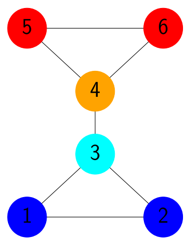

$$\boldsymbol{A} = \begin{pmatrix} 0 & 1 & 1 & 0 & 0 & 0 \\ 1 & 0 & 1 & 0 & 0 & 0 \\ 1 & 1 & 0 & 1 & 0 & 0 \\ 0 & 0 & 1 & 0 & 1 & 1 \\ 0 & 0 & 0 & 1 & 0 & 1 \\ 0 & 0 & 0 & 1 & 1 & 0 \end{pmatrix}$$

$$\boldsymbol{KLK} = \begin{pmatrix} 1.0 & -0.5 & -0.5 & 0.0 & 0.0 & 0.0 \\ -0.5 & 1.0 & -0.5 & 0.0 & 0.0 & 0.0 \\ -0.33 & -0.33 & 1.0 & -0.33 & 0.0 & 0.0 \\ 0.0 & 0.0 & -0.33 & 1.0 & -0.33 & -0.33 \\ 0.0 & 0.0 & 0.0 & -0.5 & 1.0 & -0.5 \\ 0.0 & 0.0 & 0.0 & -0.5 & -0.5 & 1.0 \end{pmatrix}$$

$$\boldsymbol{\lambda} = \begin{pmatrix} 0.00 & 0.20 & 1.17 & 1.50 & 1.63 & 1.50 \end{pmatrix}$$

$$Q = \begin{pmatrix} 0.41 & 0.46 & -0.36 & 0.71 & 0.27 & 0.16 \\ 0.41 & 0.46 & -0.36 & -0.71 & 0.27 & -0.16 \\ 0.41 & 0.27 & 0.49 & 0.0 & -0.6 & 0.0 \\ 0.41 & -0.27 & 0.49 & 0.0 & 0.6 & 0.0 \\ 0.41 & -0.46 & -0.36 & 0.0 & -0.27 & 0.69 \\ 0.41 & -0.46 & -0.36 & 0.0 & -0.27 & -0.69 \end{pmatrix}$$

$$Q^{-1} = \begin{pmatrix} 0.35 & 0.35 & 0.52 & 0.52 & 0.35 & 0.35 \\ 0.43 & 0.43 & 0.38 & -0.38 & -0.43 & -0.43 \\ -0.29 & -0.29 & 0.59 & 0.59 & -0.29 & -0.29 \\ 0.71 & -0.71 & 0.0 & 0.0 & -0.17 & 0.17 \\ 0.2 & 0.2 & -0.66 & 0.66 & -0.2 & -0.2 \\ 0.0 & 0.0 & 0.0 & 0.0 & 0.73 & -0.73 \end{pmatrix}$$

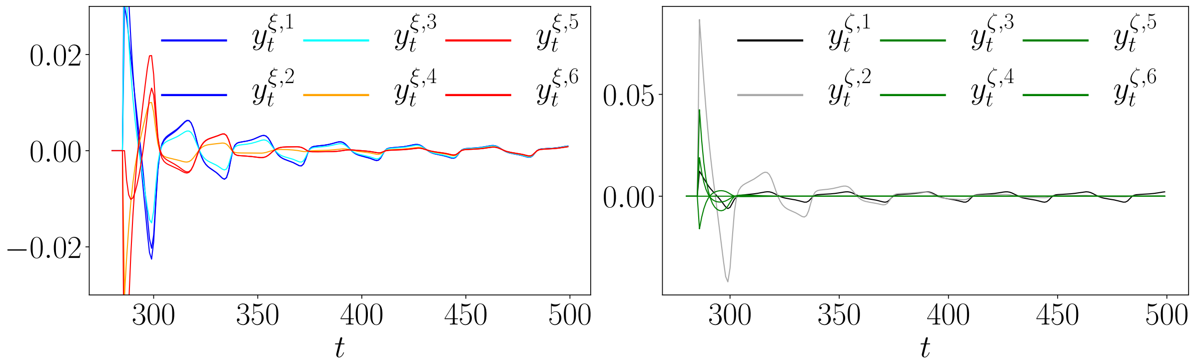

Figure 11: Complete synchronization in a network with six agents and two cliques of three nodes each. The top part of the figure shows the network, the adjacency matrix $\boldsymbol{A}$ and the normalized Laplacian $\boldsymbol{KLK}$. It also shows the eigenvalues $\boldsymbol{\lambda}$ and the eigenvectors $\boldsymbol{Q}$ of the normalized Laplacian, in a way that each column of $\boldsymbol{Q}$ is the eigenvector corresponding to the eigenvalue above. It finally shows the inverse matrix of eigenvectors $\boldsymbol{Q}^{-1}$. The bottom part of the figure shows the evolution of the deviations in the original basis and in the eigenbasis.

for the red and orange lines ($t = 292$), the dark green and light green lines ($t = 303$) and purple and pink lines ($t = 309$). As discussed in Section 5.1.1, shocks have strongest desynchronizing effects during a recession or during a growth period. The desynchronizing effect in a trough is smaller, while the effect at a peak is minimal. It is interesting that most of the differences are due to the first eigenmode, while the evolution of the second eigenmode is almost independent of timing.

It is also interesting that the strongest desynchronizing effect occurs during a recession rather than during a boom (blue vs dark green line). This can be explained from Figure 7b, noting that a recession is followed by a trough, where the Lyapunov exponent is smaller but not minimal; on the other contrary, a boom is followed by a peak, where the Lyapunov exponent is minimal. Even if the shock occurs at times in which the Lyapunov exponent is identical, the evolution of the deviation is affected differently in the two cases. The dark green line shows how the shock is suddenly dampened, corresponding to dynamics reaching the peak. The blue line, on the other hand, shows that the shock is not as much dampened, because dynamics reach the trough where the Lyapunov exponent is not minimal.

Six agents with two cliques of three nodes each. To understand the effect of the network structure on shock propagation and synchronizing non-linear dynamics, we consider the network in Figure 11. This network is composed of two cliques of three nodes each, connected by a link between two of the nodes of the cliques. These two nodes are colored lighter to highlight the stronger connectivity to the other clique. This network can be thought of as a stylized model of sectors in two countries, as will be clear in the following input-output interpretation of the model (Section 5.2).

At time $\tau = 285$, we apply the following shock vector:

$$\left(y_{\tau+1}^{\xi,1}, y_{\tau+1}^{\xi,2}, y_{\tau+1}^{\xi,3}, y_{\tau+1}^{\xi,4}, y_{\tau+1}^{\xi,5}, y_{\tau+1}^{\xi,6}\right) = (0.05, 0.03, 0.04, -0.03, -0.06, 0.00). \qquad (17)$$

This shock vector can be thought of as idiosyncratic shocks hitting all agents differently, combined with a positive shock hitting the clique with agents 1,2 and 3, and a negative shock hitting the other clique. In the eigenbasis, this shock vector corresponds to

$$\left(y^{\zeta,1}_{\tau+1}, y^{\zeta,2}_{\tau+1}, y^{\zeta,3}_{\tau+1}, y^{\zeta,4}_{\tau+1}, y^{\zeta,5}_{\tau+1}, y^{\zeta,6}_{\tau+1}\right) = (0.01, 0.09, 0.00, 0.02, -0.02, -0.04). \tag{18}$$

It is already clear that positive shocks in the first clique and negative shocks in the second clique make the initial condition of the second eigenmode (0.09) the largest one.

The evolution of shocks is shown at the bottom of Figure 11. In the panel on the left, we show the shocks in the original basis, i.e. each line corresponds to an agent. It is clear that dynamics vary across the two cliques, but they are very similar within any of the two cliques. The cyan and orange lines, corresponding to the two "bridge" agents, are the ones that are most similar to dynamics in the other clique. Over time, all dynamics converge again to the synchronized state, with a permanent phase shift.

The evolution of shocks in the eigenbasis is shown in the right panel. The black line is the eigenmode which is parallel to the synchronization manifold. The grey line corresponds to the second eigenmode, the one with largest initial value, and decays very slowly. The green lines correspond to the third to sixth eigenvectors, and decay very quickly.

The interpretation for the eigenmodes is now clear. The second eigenmode corresponds to synchronization across cliques. Indeed, because $y^{\zeta,2}_t = 0.43y^{\xi,1}_t + 0.43y^{\xi,2}_t + 0.38y^{\xi,3}_t - 0.38y^{\xi,4}_t - 0.43y^{\xi,5}_t - 0.43y^{\xi,6}_t$, it is maximal in absolute value when shocks are positive in one clique and negative in the other one. This eigenmode takes time to decay, because the eigenvalue λ_2 is relatively small and so, as shown in Figure 7a, the Lyapunov exponent is not very negative. This means that synchronization across cliques takes time. The third to sixth eigenmodes correspond to synchronization within cliques, and decay very quickly ($K = \epsilon\lambda_i$, $i = 3, \dots 6$ is relatively large, so the Lyapunov exponent is more negative than in the case of $K = \epsilon\lambda_2$). This indicates that synchronization within cliques happens very quickly.

This phenomenon is general, because the second eigenvector of the Laplacian—the Fiedler vector—takes positive values in a cluster of nodes, and negative values in the other one. If there were M cliques, or more loosely M clusters of highly connected nodes, weakly connected across one another, there would be $M-1$ small eigenvalues and then a large gap to the next eigenvalue. The eigenmodes corresponding to the small eigenvalues would indicate, as in the case above, synchronization across clusters. The remaining $N - M$ eigenvalues would be much larger, and the associated eigenmodes would correspond to synchronization within clusters.[25]

5.2 Input-output business cycle model

The analysis above was performed for unweighted, undirected networks. These have the convenient mathematical property that all eigenvalues of the normalized Laplacian are real, positive and bounded between zero and two. In the case of directed, weighted networks, with connectivity matrix $\boldsymbol{W}$ (so that all rows are normalized to one), instead of calculating the eigenvalues of $\boldsymbol{KLK}$ one calculates those of $\boldsymbol{I}_N - \boldsymbol{W}$. The analysis is similar, but the eigenvalues could be complex.[26] In practice, with the input-output networks that we consider, the imaginary part of eigenvalues and eigenvectors is negligible, so that the analysis is very similar to the previous case.

As an illustration, in Figure 12 we consider a number of mostly negative shocks hitting all economic sectors in Belgium and the Netherlands. These two countries are chosen as

[25] There could also be a hierarchy of clusters. Imagine for example that there were two main clusters, and two sub-clusters within each cluster. Here, the Fiedler vector would divide between the two main clusters, but then the following eigenmode (corresponding to a larger eigenvalue) would correspond to synchronization between sub-clusters. There would be a time-scale separation so that synchronization would first occur within sub-clusters, then across sub-clusters within the same main cluster, and finally across main clusters.

[26] Applying master stability analysis in the case of complex eigenvalues is almost identical to the case of real eigenvalues, except that one computes complex Floquet exponents (instead of real Lyapunov exponents) and then verifies if the complex values of $K = \epsilon\lambda_i$ are inside the stable region in the complex plane.

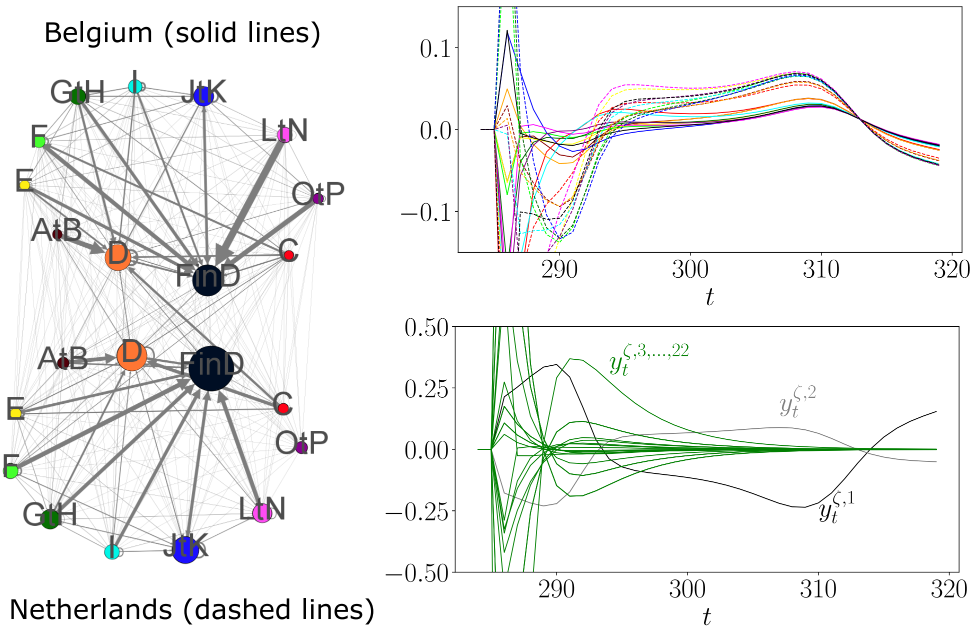

Figure 12: Complete synchronization in the Belgium-Netherlands input-output network. Left Panel: The node size is proportional to the total value of sector-country pairs or final demand. Links are the value flows (goods and services flow in the same direction as the arrow) and their size is proportional to the value of these flows normalized by the total output of the node. AtB: Agriculture; C: Mining; D: Manufacturing; E: Utilities; F: Construction; GtH: Trade; I: Transports; JtK: Finance and other business services; LtN: Government services; OtP: Other services; FinD: Final demand. Right panel: The lines in the top right panel are colored as the nodes in the input-output network. Solid lines correspond to Belgian sectors, while dashed lines correspond to Dutch sectors.

their output is of the same order of magnitude and, being relatively small, their openness to other countries is larger than in the case of big countries. The input-output network is shown on the left. It is composed of $N = 22$ nodes, 10 economic sectors in each country and final demand in each country. The sectors that are mostly connected to the other country are AtB: Agriculture, C: Mining and D: Manufacturing. Final demand acts as a central hub within each country (the edges from final demand to the other sectors, proportional to the pointed sector's size, are only visible in the case of the "JtK: Finance and other business services" sector).

In the top right panel we show dynamics after the shocks. The solid and dashed lines quickly cluster into two distinct groups, indicating that synchronization is quickly reached within each country, but it takes longer to reach synchronization across the two countries. Interestingly, the sectors whose dynamics are closest to the other country's average dynamics are agriculture, mining and manufacturing, which act as bridges between the two countries (see the dark red, red and orange lines). Since agriculture and mining are tiny as compared to manufacturing, one can say that manufacturing is the most important connection between the two countries.

In the bottom right panel we show dynamics in the eigenbasis. The eigenvalues of $\boldsymbol{I}_{22} - \boldsymbol{W}$ are $\lambda_1 = 0$, $\lambda_2 = 0.09$, $\lambda_{3,\ldots,N} \geq 0.77$.[27] The large gap between λ_2 and λ_3 indicates that the network is strongly clustered into two groups, as was evident in Figure 12. The Fiedler eigenvector, corresponding to λ_2, is

$$\boldsymbol{v}_2 = (-0.15, -0.17, -0.15, -0.25, -0.29, -0.25, -0.23, -0.26, -0.29, -0.28, -0.27, \\ 0.11, 0.04, 0.09, 0.2, 0.23, 0.19, 0.18, 0.21, 0.22, 0.21, 0.20). \tag{19}$$

[27] Some eigenvalues have a small imaginary part. The eigenvalues with largest imaginary part are $\lambda_\pm = 0.77 \pm 0.06j$, suggesting that the real part is dominating. Simulations suggest that it should be safe to simply ignore the imaginary part.

This also shows a division into two communities. The first 11 components of this vector correspond to Belgium and are negative, while the final 11 components correspond to the Netherlands and are positive. The first three components—corresponding to agriculture, mining and manufacturing—are less negative, exactly like the first three positive components (0.11, 0.04, 0.09) which are less positive. This indicates that these sectors are "closer" to sectors in the other country. It also explains why the red and orange lines are close to one another in the top right panel of Figure 12. Because after some time only the first and second eigenmodes matter, and the first eigenmode is identical for all units, one can focus on the second eigenmode to understand the relative dynamics of the units. The deviations $y_t^{\xi,i}$ are simply proportional to the component of the Fiedler vector, and so indeed units whose components are closer in value to units in the other cluster can be expected to have closer dynamics.

Given that the spectral properties of the network are very similar to the example in Section 5.1, with two cliques of three nodes each, it is not surprising that dynamics are similar. The eigenmodes corresponding to eigenvalues λ_i, $i \geq 3$, decay very quickly, while the eigenmode corresponding to λ_2 decays more slowly. This is consistent with the pattern described above by which synchronization within each country is reached quickly, while synchronization across countries takes longer.

We finally consider the international input-output network in which we aggregate all sectors within a country, as we did in Section 4.2. This is a network with $N = 17$ nodes, whose weight matrix $\boldsymbol{W}$ is shown in Table 2. The eigenvalues of $\boldsymbol{I}_{17} - \boldsymbol{W}$ are: $\lambda_1 = 0.0$; $\lambda_2 = 0.04$; $\lambda_3 = 0.06$; $\lambda_4 = 0.08$; $\lambda_5 = 0.15$; $\lambda_6 = 0.16$; $\lambda_7 = 0.18$; $\lambda_8 = 0.2$; $\lambda_9 = 0.22$; $\lambda_{10} = 0.26$; $\lambda_{11} = 0.33$; $\lambda_{12} = 0.36$; $\lambda_{13} = 0.36$; $\lambda_{14} = 0.36$; $\lambda_{15} = 0.37$; $\lambda_{16} = 0.47$; $\lambda_{17} = 0.52$. It is clear that these eigenvalues are much smaller than the ones corresponding to the sectoral input-output network in Belgium and the Netherlands. This means that synchronization takes longer in this network, as one could expect based on how small the international linkages are relative to the national ones. Moreover, as there are no clear gaps between groups of eigenvalues, there is no clear hierarchical structure in terms of clusters or communities. This is confirmed by simulations (not reported).

It is also interesting to consider the components of the Fiedler vector. These are, with the respective country: JPN: -0.66; AUS: -0.43; CAN: 0.05; USA: 0.06; IRL: 0.1; DNK: 0.13; SWE: 0.13; FIN: 0.14; GBR: 0.14; NLD: 0.16; BEL: 0.16; DEU: 0.17; AUT: 0.17; FRA: 0.19; ITA: 0.21; PRT: 0.22; ESP: 0.23. These values clearly shows geographical and cultural patterns, and give a first approximation to which countries are likely to be most strongly correlated to one another. (For this reason, the Fiedler vector is commonly used in spectral community detection.)

6 Empirical application

The theory of complete synchronization developed in Section 5 is particularly useful to explain how synchronization theory could improve on existing exogenous business cycle models in terms of generating higher comovement between economic time series.

Consider two agents following two deterministic identical limit cycles in isolation. When coupled, absent shocks, after some time their dynamics perfectly align in the synchronized state $\boldsymbol{s}_t = (x_t^s, y_t^s)$. Suppose now that at time t, the decision variables y^i of the agents are hit by idiosyncratic shocks ξ_t^1 and ξ_t^2. The comovement between time series of the decision variables, calculated for the time steps immediately following the shocks, is given by the Pearson correlation coefficient

$$\operatorname{cor}\left(y_t^s + \xi_t^1, y_t^s + \xi_t^2\right) = \frac{\operatorname{cov}\left(y_t^s, y_t^s\right) + \operatorname{cov}\left(y_t^s, \xi_t^2\right) + \operatorname{cov}\left(\xi_t^1, y_t^s\right) + \operatorname{cov}\left(\xi_t^1, \xi_t^2\right)}{\operatorname{std}\left(y_t^s + \xi_t^1\right) \cdot \operatorname{std}\left(y_t^s + \xi_t^2\right)}. \tag{20}$$

In the above equation, cov denotes the covariance, std indicates the standard deviation, and we have used linearity of the covariance to decompose it in various terms. Compare this equation with the correlation between time series of two agents that are in the same stable steady state and are hit by shocks (ξ_t^1, ξ_t^2):

$$\text{cor}\left(\xi_t^1, \xi_t^2\right) = \frac{\text{cov}\left(\xi_t^1, \xi_t^2\right)}{\text{std}\left(\xi_t^1\right) \cdot \text{std}\left(\xi_t^2\right)}. \tag{21}$$

If we assume that the variance of endogenous and exogenous fluctuations is the same (i.e. fluctuations have the same intensity), the correlation coefficient is only determined by the numerators of these expressions. Comparing Eq. (20) and Eq. (21), it is clear that the endogenous component of dynamics potentially increases correlation. In particular, when the variance of the shocks is small relative to the variance of y_t^s, the correlation coefficient tends to one in the first case.

In the following, we perform simulations to show that comovement produced by endogenous fluctuations is systematically larger than in the case of exogenous fluctuations, even when shocks repeatedly hit agents. We also show that endogenous fluctuations give greater flexibility in matching the heterogeneity of correlations in the data. In Section 6.1, we first give a quick description of the data (more details in Appendix A), we then compare data to simulations in Section 6.2.

6.1 Data

6.1.1 World Input-Output Database

We calibrate interaction coefficients in the input-output specification of our model using the World Input-Output Database (Timmer et al., 2015). This database integrates several national input-output tables in a coherent way, detailing value flows of intermediate and final goods across sector-country pairs. Although data are available yearly between 1995 and 2011, we only use data for year 2000. This arbitrary choice reflects our simplifying assumption of a fixed input-output network. In any case, input-output networks evolve very slowly, so our results are likely not sensitive to this choice. For compatibility with other data sources, we focus on 17 countries and 27 sectors within each country, and we use the 2013 release, which classifies sectors according to ISIC Rev. 3. (See Section 6.1.2 and Appendix A.)

Here, we simply highlight a property of these data. Following the procedure described in Section 3.2, we construct the graph with interaction matrix $\boldsymbol{W}$, which is composed of $N = 17 \cdot 28 = 476$ nodes, including final demand nodes. We then calculate the eigenvalues of $\boldsymbol{I}_{476} - \boldsymbol{W}$, take their real part (the imaginary part is negligible), sort them, and show them in Figure 13 (blue dots). One can see 17 eigenvalues close to zero, 17 eigenvalues close to 1.5, and all other eigenvalues between 0.7 and 1.1. We compare this spectrum to the spectrum of a collection of 17 star networks of 28 nodes each, connected to one another through their central nodes (in other words, the central nodes form a complete graph). As one can see, the two spectra are qualitatively similar.

This result indicates that the network structure shown in Figure 12 is in fact common across countries, having final demand as their central node. Moreover, countries are relatively isolated, with only a few sectors acting as bridges. Some of these network properties will be reflected in time series patterns, to which we now turn.

6.1.2 Time series data

To study synchronization of business cycles across sectors and countries, we create a novel dataset that is designed to have the broadest possible coverage on four dimensions: length of time series, sectoral disaggregation of the economy, number of countries sufficiently similar to one another, and coverage of the most important macroeconomic variables. In Appendix A, we describe how we assemble a dataset starting from five primary databases: KLEMS, OECD STAN, OECD ISDB, UNIDO INDSTAT and GGDC 10-sector. Each of these databases, individually, either has too short time series (to study business cycles, it is crucial to have as long time series as possible), too few countries or variables or too aggregate sectors. By merging these datasets, we achieve the best compromise on these dimensions. Although we

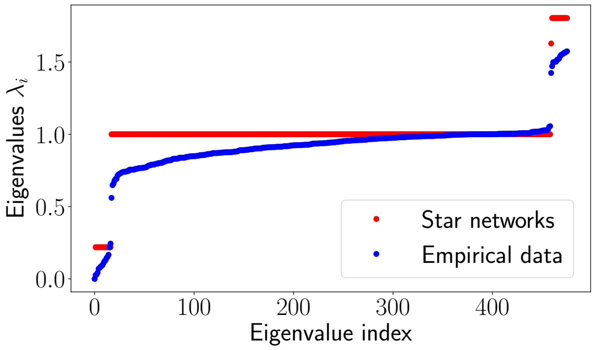

Figure 13: Spectrum of the interaction matrix $\boldsymbol{W}$ built from the World Input-Output Database (blue dots), compared to the spectrum of the normalized Laplacian $\boldsymbol{KLK}$ of a collection of star networks connected by their central nodes (red dots).

collected other variables, in this paper we focus on employment and real GDP as business cycle indicators. Data are available yearly in the period 1960-2016, across 27 disaggregate sectors and 9 sector aggregates, for 17 advanced economies (US, Canada, Australia, Japan and 13 European countries). See Appendix A for the full list of countries and sectors and for information about missing data.

Employment (number of persons employed—employees and self-employed) has the main advantage that it is trendless in the aggregate, so that business cycle fluctuations are not contaminated by a trend (Beaudry et al., 2020). However, we are interested in sectoral dynamics, which follows business cycles together with long-term trends, such as the secular decline in the labor share of manufacturing. Moreover, we also want to compare to real GDP, which has a trend both in the aggregate and across sectors. Using growth rates to obtain stationary time series does not appear appropriate to us, as yearly growth rates mask low frequency movements which are a key property of endogenous business cycle models. We resorted to using the filter proposed by Christiano and Fitzgerald (2003) (CF), which is a band-pass filter that only keeps fluctuations in a certain range. To be as inclusive as possible, we only remove fluctuations of periodicity lower than 2 years or greater than 25 years. As a business cycle indicator, we consider the ratio between the cyclic and trend components produced by the filter.

In Figure 14, we show pairwise correlation coefficients across 27 disaggregate sectors in the US and across 17 national aggregates. It is immediately clear that AtB-Agriculture, C-Mining, E-Utilities, government sectors (L-Public administration, M-Education, N-Health) and P–Private households with employed persons– are uncorrelated, or even negatively correlated, to other sectors and with themselves.[28] This result could be expected: sectors such as agriculture, mining and utilities are highly affected by exogenous factors, and governments following countercyclical policies are by definition uncorrelated or anticorrelated with the cycle. On the contrary, manufacturing sectors are highly correlated, together with F-Construction, G-Trade, H-Restaurant and hotels, K7174-Business services and O-Community services. When it comes to countries, it can be observed that the highest pairwise correlation occurs between the US and Canada, and that there is not a clear difference between European countries and the US, Canada, Australia and Japan. This can be explained by the fact that these correlation coefficients are calculated starting 1960, well before the convergence that started in the nineties (see Figure 1, top right panel). In Appendix B, Figures 17 and 18, we show additional pairwise correlation data. These give a visual impression of the fact that correlations are stronger within than across countries, and that the sectors that are most correlated internationally are manufacturing, construction, trade, transports and business services.

[28]In these US data, K70-Real estate has the same level of correlation, but this is untypical.

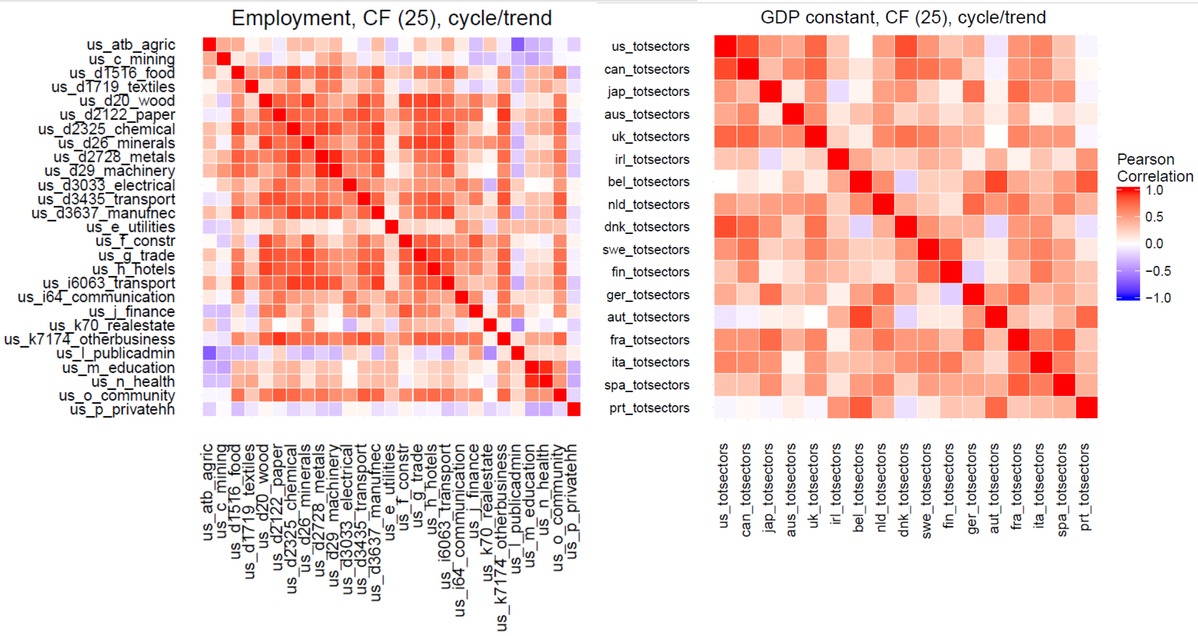

Figure 14: Pairwise Pearson correlation coefficients across 27 sectors in the US economy, and across 17 national aggregates. Data are detrended with a CF filter, and we consider the ratio between cycle and trend.

6.2 Analysis

Our theoretical analysis so far was performed with reference to a single shock hitting one or more agents/sector-country pairs at a given time step. Of course, in reality shocks repeatedly hit economic agents. These shocks can have a rich structure, such as heterogeneous variance, autocorrelation, and correlation structure. Our empirical analysis in Section 6.1.2 above shows that some sectors are clearly less correlated to the others—most likely, they are hit by idiosyncratic shocks with relatively large variance. Moreover, idiosyncratic shocks are certainly complemented by common shocks, whether at the sector or country level.

To properly compare the predictions of our model to data is out of the scope of the present work, which is mainly an illustration of the potential of synchronization theory to explain comovement. On one hand, it would be necessary to identify idiosyncratic, sector-specific and country-specific shock processes. On the other hand, one should use a structural model with a clear map to economic variables, rather than an abstract reduced-form model as we do. Nevertheless, we attempt to compare our results to data, to see how far we can go.

We choose all parameters as in the previous sections, except for the ones that we vary to obtain three scenarios for the deterministic dynamics, and three scenarios for shocks. Because we want to compare endogenous and exogenous business cycle models, we consider a scenario in which deterministic dynamics follow a limit cycle ($\alpha_1 = -0.04$, $\alpha_2 = 0.4$, $\delta = 0.1$), together with two scenarios in which they converge to a steady state. The difference between these two latter scenarios is in how they converge. In one case the steady state is a node, i.e. the eigenvalues of the Jacobian are real and dynamics converges without oscillations ($\alpha_1 = -0.11$, $\alpha_2 = 0.4$, $\delta = 0.5$). In the second case the fixed point is a focus, with complex eigenvalues and dampened oscillations ($\alpha_1 = -0.04$, $\alpha_2 = 0.3$, $\delta = 0.1$). The three scenarios for shocks explore the interplay between idiosyncratic, sectoral and national shocks. In the idiosyncratic scenario, only the standard deviation of the sector-country-specific shock process is positive ($\sigma_u > 0$, $\sigma_v = 0$, $\sigma_z = 0$), in the scenario with country-specific shocks both σ_u and σ_z are positive, and in the scenario with sector-specific shocks, σ_u and σ_v are positive. In all cases, we assume that idiosyncratic shocks have no persistence ($\rho_u = 0$), while sector- and country-specific shocks have weak persistence ($\rho_v = \rho_z = 0.3$). In all cases, finally, all standard deviations and persistence parameters are identical across agents.

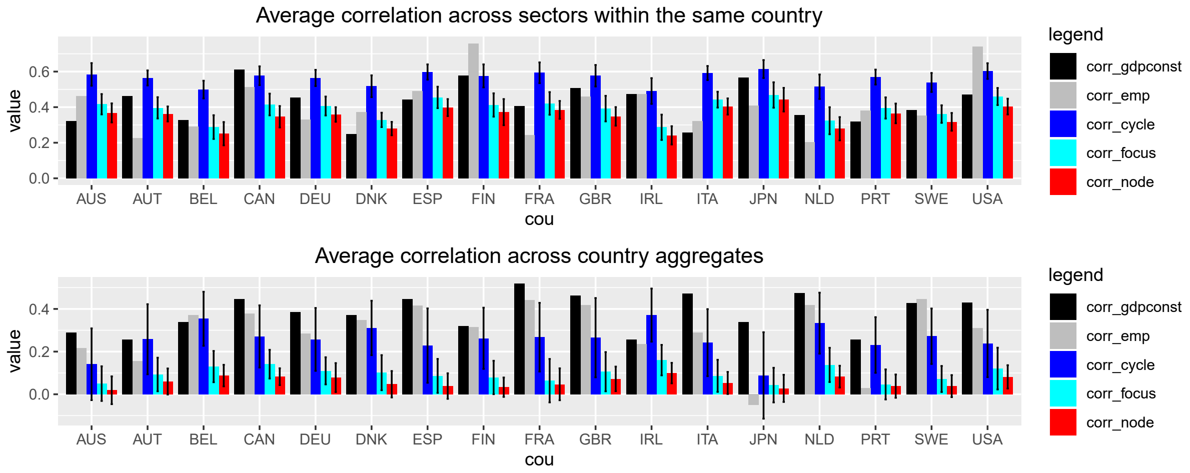

Figure 15: Comparison of average correlation coefficients between empirical data and the three deterministic scenarios of the model. In the top panel, we calculate the average of sectoral pairwise correlation coefficients within the same country, for all countries. In the bottom panel, we calculate all pairwise correlation coefficients between country aggregates, and then average all those involving any given country. Error bars correspond to one standard deviation, computed over 20 realizations of the model.

We simulate our model for the full set of 27 sectors and 17 countries. Simulations last 600 time steps, which we interpret as quarters. This choice makes sense as the period of the cycle with the parameters above is 36 quarters, in line with empirical evidence (Beaudry et al., 2020). We only retain the last 228 time steps, and average them so as to produce 57 yearly observations (our empirical data run 1960-2016). For each combination of parameters, we run our model with 20 different random seeds to account for stochasticity.

Because we do not have a structural model with estimated shock processes, we need to make some assumptions concerning the comparison with data. First of all, we reduce the number of sectors, by aggregating simulated data to 10 sectors (the ones listed in Table 1). Second, rather than predicting individual correlation coefficients, we consider averages within and across countries—see below. Third, we drop agriculture, mining, utilities and government. As we noted in Figure 14, these seem to move independently from the rest of the economy. Because we do not model the government, it makes sense to exclude it, while the three other sectors make up less than 5% of the economy, but can have a large weight in determining average correlation coefficients as an artifact of how these are computed.

In Figure 15, we perform a first comparison of the predictions of our model to data. We consider all three scenarios for deterministic dynamics—cycle, focus and node—, but we just consider idiosyncratic shocks, with standard deviation $\sigma_u = 0.24$. Several results are worth mentioning. First of all, correlation produced by cycles is always larger than correlation under focus or node parameterizations. This effect is much stronger when comparing country aggregates, but it is also noticeable across sectors within the same country. Second, countries with relatively high correlations for the cycle scenario tend to have relatively high correlations for focus and node scenarios, too, but there is not much variability in the level of correlations across countries within the same scenario. Third, error bars are quite small within countries, but large across countries. Forth, for sectors within countries it is not clear which scenario best explains empirical correlations, as it varies by country, but when considering country aggregates only endogenous fluctuations can account for the empirical comovement. In other words—for this level of σ_u—both endogenous and exogenous fluctuations can account for comovement across sectors, but only endogenous fluctuations can account for international comovement.

How general are these results? In Figure 16 we perform more extensive numerical experiments, by considering at the same time the three scenarios for deterministic dynamics and the three scenarios for shock processes. In all cases, we vary the standard deviation

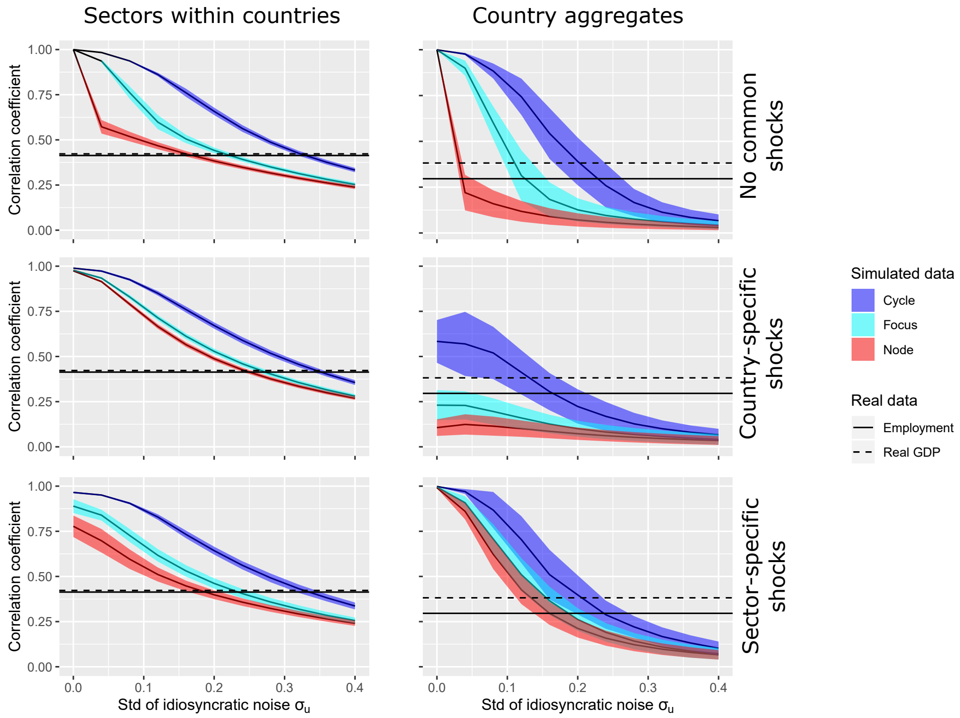

Figure 16: Comparison of average correlation coefficients between empirical data and all combinations of scenarios for deterministic dynamics and shock processes. In left panels, we compute averages across all sectors within the same country, and then across all countries; in right panels, we average all pairwise correlation coefficients across country aggregates. Colored bands indicate one standard deviation, computed across 20 realization of the model.

of idiosyncratic noise σ_u between 0 and 0.4; in case of country-specific shocks, we also set $\sigma_z = 0.05$, while in case of sector-specific shocks, we set $\sigma_v = 0.05$.

As in Figure 15, endogenous fluctuations always produce more comovement than exogenous ones. In all cases except one, there exists a value of σ_u under which any deterministic scenario can match the level of comovement in the data. Within countries, when noise is weak, exogenous fluctuations seem to better match empirical comovement, but they generate too low comovement when noise is stronger. Across counties, exogenous fluctuations are able to generate sufficiently high comovement only in case of sector-specific shocks. Overall, this confirms the intuition in Figure 15, that exogenous fluctuations can go some way into explaining sectoral comovement within countries, but endogenous fluctuations seem to be much better suited to explain international comovement.

These results come with two caveats. First, some of the pairwise correlation coefficients shown in Figures 14, 17 and 18 are much larger than the averages shown in Figure 16, while other correlations are much smaller. To account for this variety, it is useful to consider all three deterministic scenarios. Second, while we believe that endogenous fluctuations would produce stronger comovement than exogenous fluctuations independently of the model being used, we do not claim that the *level* of correlations is model independent. For example, another model might produce weaker sectoral movement in all cases, requiring endogenous fluctuations to match the empirical level of sectoral comovement, too.

7 Conclusion

In a popular science book, Krugman (1996) wrote: "One of the luxuries of a format like this one is that I can include the kind of loose speculations that I could never write in a journal and that I can explain, as I am doing now, that I do not necessarily believe in the theory I am advancing. So here is a crazy idea about the global business cycle: it is an example of "phase locking."[...] Like the two back-to-back clocks that started ticking in unison, the two economies would not need to be very strongly linked to develop a synchronized cycle; a modest linkage would do as long as they were predisposed to have cycles in any case and had fairly similar natural periods." In this paper, we dare exploring this hypothesis, showing that it is highly promising to explain comovement of business cycles across sectors and countries.

Our work can be extended in several ways. First of all, it would be interesting to apply the methods that we introduce in this paper to other models, for example microfounded business cycle models that attribute fluctuations to specific economic forces and microfounded shocks. In parallel, it would be interesting to explore other channels for synchronization, such as financial linkages, multinational corporate control, and animal spirits. To do that, one would need to further disaggregate agents, and study how individual firms and households would synchronize their dynamics. Within macroeconomics, our framework can also be extended to study comovement across regions, and it could be coupled with the (slow) evolution of the input-output network. Beyond macroeconomics, we hope that the tools that we offer in this paper can find wider applicability, as any disaggregate dynamic model that can be described by some form of non-linear dynamics can be studied with the tools of synchronization theory.

8 Bibliography

Acemoglu, D., Carvalho, V. M., Ozdaglar, A., and Tahbaz-Salehi, A. (2012) "The network origins of aggregate fluctuations," *Econometrica*, Vol. 80, pp. 1977–2016.

Arenas, A., Díaz-Guilera, A., Kurths, J., Moreno, Y., and Zhou, C. (2008) "Synchronization in complex networks," *Physics Reports*, Vol. 469, pp. 93–153.

Arkolakis, C. and Ramanarayanan, A. (2009) "Vertical specialization and international business cycle synchronization," *Scandinavian Journal of Economics*, Vol. 111, pp. 655–680.

Backus, D. K., Kehoe, P. J., and Kydland, F. E. (1992) "International real business cycles," *Journal of Political Economy*, Vol. 100, pp. 745–775.

Baqaee, D. R. and Farhi, E. (2019) "The macroeconomic impact of microeconomic shocks: beyond Hulten's Theorem," *Econometrica*, Vol. 87, pp. 1155–1203.

Barahona, M. and Pecora, L. M. (2002) "Synchronization in small-world systems," *Physical Review Letters*, Vol. 89, p. 054101.

Barnett, W. A. and Chen, P. (1988) "The aggregation-theoretic monetary aggregates are chaotic and have strange attractors," in W. A. Barnett, E. R. Berndt, and H. White eds. *Dynamic Econometric Modeling*: Cambridge University Press, pp. 199–246.

Barnett, W. A. and Serletis, A. (2000) "Martingales, nonlinearity, and chaos," *Journal of Economic Dynamics and Control*, Vol. 24, pp. 703–724.

Baxter, M. and Kouparitsas, M. A. (2005) "Determinants of business cycle comovement: a robust analysis," *Journal of Monetary Economics*, Vol. 52, pp. 113–157.

Beaudry, P., Galizia, D., and Portier, F. (2015) "Reviving the Limit Cycle View of Macroeconomic Fluctuations,"Technical report, National Bureau of Economic Research.

——— (2020) "Putting the Cycle Back into Business Cycle Analysis," *American Economic Review*, Vol. 110, pp. 1–47.

Boldrin, M. and Woodford, M. (1990) "Equilibrium models displaying endogenous fluctuations and chaos: a survey," *Journal of Monetary Economics*, Vol. 25, pp. 189–222.

Bramoullé, Y., Galeotti, A., and Rogers, B. (2016) *The Oxford handbook of the economics of networks*: Oxford University Press.

Brenner, T., Weidlich, W., and Witt, U. (2002) "International Co-movements of Business Cycles in a "Phase-locking" Model," *Metroeconomica*, Vol. 53, pp. 113–138.

Brock, W. A. (1986) "Distinguishing random and deterministic systems: Abridged version," *Journal of Economic Theory*, Vol. 40, pp. 168–195.

Bullard, J. (1994) "Learning equilibria," *Journal of Economic Theory*, Vol. 64, pp. 468–485.

Bulow, J. I., Geanakoplos, J. D., and Klemperer, P. D. (1985) "Multimarket oligopoly: Strategic substitutes and complements," *Journal of Political Economy*, Vol. 93, pp. 488–511.

Calderon, C., Chong, A., and Stein, E. (2007) "Trade intensity and business cycle synchronization: Are developing countries any different?" *Journal of International Economics*, Vol. 71, pp. 2–21.

Carvalho, V. M. (2014) "From micro to macro via production networks," *Journal of Economic Perspectives*, Vol. 28, pp. 23–48.

Cerina, F., Zhu, Z., Chessa, A., and Riccaboni, M. (2015) "World input-output network," *PloS One*, Vol. 10, p. e0134025.

Christiano, L. J. and Fitzgerald, T. J. (2003) "The band pass filter," *International Economic Review*, Vol. 44, pp. 435–465.

Cooper, R. and Haltiwanger, J. (1990) "Inventories and the propagation of sectoral shocks," *American Economic Review*, pp. 170–190.

Cooper, R. and John, A. (1988) "Coordinating coordination failures in Keynesian models," *Quarterly Journal of Economics*, pp. 441–463.

Cravino, J. and Levchenko, A. A. (2017) "Multinational firms and international business cycle transmission," *Quarterly Journal of Economics*, Vol. 132, pp. 921–962.

Dawid, H. and Delli Gatti, D. (2018) "Agent-based macroeconomics," in *Handbook of Computational Economics*, Vol. 4: Elsevier, pp. 63–156.

De Grauwe, P. (2011) "Animal spirits and monetary policy," *Economic Theory*, Vol. 47, pp. 423–457.

Di Giovanni, J. and Levchenko, A. A. (2010) "Putting the parts together: trade, vertical linkages, and business cycle comovement," *American Economic Journal: Macroeconomics*, Vol. 2, pp. 95–124.

Di Giovanni, J., Levchenko, A. A., and Mejean, I. (2018) "The micro origins of international business-cycle comovement," *American Economic Review*, Vol. 108, pp. 82–108.

Fazzari, S., Ferri, P., and Greenberg, E. (2008) "Cash flow, investment, and Keynes–Minsky cycles," *Journal of Economic Behavior & Organization*, Vol. 65, pp. 555–572.

Foerster, A. T., Sarte, P.-D. G., and Watson, M. W. (2011) "Sectoral versus aggregate shocks: A structural factor analysis of industrial production," *Journal of Political Economy*, Vol. 119, pp. 1–38.

Foley, D. K. (1992) "A contribution to the theory of business cycles," *Quarterly Journal of Economics*, Vol. 107, pp. 1071–1088.

Forni, M. and Reichlin, L. (1998) "Let's get real: a factor analytical approach to disaggregated business cycle dynamics," *Review of Economic Studies*, Vol. 65, pp. 453–473.

Frankel, J. A. and Rose, A. K. (1998) "The endogenity of the optimum currency area criteria," *Economic Journal*, Vol. 108, pp. 1009–1025.

Goodwin, R. M. (1951) "The nonlinear accelerator and the persistence of business cycles," *Econometrica*, pp. 1–17.

——— (1967) *A Growth Cycle*: Cambridge University Press.

Granger, C. W. (1966) "The typical spectral shape of an economic variable," *Econometrica*, pp. 150–161.

Gualdi, S., Bouchaud, J.-P., Cencetti, G., Tarzia, M., and Zamponi, F. (2015) "Endogenous crisis waves: stochastic model with synchronized collective behavior," *Physical Review Letters*, Vol. 114, p. 088701.

Haxholdt, C., Kampmann, C., Mosekilde, E., and Sterman, J. D. (1995) "Mode-locking and entrainment of endogenous economic cycles," *System Dynamics Review*, Vol. 11, pp. 177–198.

Hicks, J. R. (1950) *A Contribution to the Theory of the Trade Cycle*: Oxford University Press.

Hommes, C. H. and Manzan, S. (2006) "Comments on "Testing for nonlinear structure and chaos in economic time series"," *Journal of Macroeconomics*, Vol. 28, pp. 169–174.

Hornstein, A. and Praschnik, J. (1997) "Intermediate inputs and sectoral comovement in the business cycle," *Journal of Monetary Economics*, Vol. 40, pp. 573–595.

Horvath, M. (1998) "Cyclicality and sectoral linkages: Aggregate fluctuations from independent sectoral shocks," *Review of Economic Dynamics*, Vol. 1, pp. 781–808.

——— (2000) "Sectoral shocks and aggregate fluctuations," *Journal of Monetary Economics*, Vol. 45, pp. 69–106.

Hsu, C.-C., Wu, J.-Y., and Yau, R. (2011) "Foreign direct investment and business cycle co-movements: The panel data evidence," *Journal of Macroeconomics*, Vol. 33, pp. 770–783.

Imbs, J. (2004) "Trade, finance, specialization, and synchronization," *Review of Economics and Statistics*, Vol. 86, pp. 723–734.

——— (2006) "The real effects of financial integration," *Journal of International Economics*, Vol. 68, pp. 296–324.

Johnson, R. C. (2014) "Trade in intermediate inputs and business cycle comovement," *American Economic Journal: Macroeconomics*, Vol. 6, pp. 39–83.

Judd, K. L. (1985) "On the performance of patents," *Econometrica*, pp. 567–585.

Kaldor, N. (1940) "A model of the trade cycle," *Economic Journal*, pp. 78–92.

Kalemli-Ozcan, S., Papaioannou, E., and Peydro, J.-L. (2013) "Financial regulation, financial globalization, and the synchronization of economic activity," *Journal of Finance*, Vol. 68, pp. 1179–1228.

Kaplan, G. and Violante, G. L. (2018) "Microeconomic heterogeneity and macroeconomic shocks," *Journal of Economic Perspectives*, Vol. 32, pp. 167–94.

Kose, M. A. and Yi, K.-M. (2006) "Can the standard international business cycle model explain the relation between trade and comovement?" *Journal of International Economics*, Vol. 68, pp. 267–295.

Krugman, P. (1996) *The self-organizing economy*: Blackwell Publishers.

Kuramoto, Y. (2003) *Chemical oscillations, waves, and turbulence*: Courier Corporation.

vom Lehn, C. and Winberry, T. (2019) "The investment network, sectoral comovement, and the changing U.S. business cycle," NBER Working Papers 26507.

Liao, W. and Santacreu, A. M. (2015) "The trade comovement puzzle and the margins of international trade," *Journal of International Economics*, Vol. 96, pp. 266–288.

Long, J. B. and Plosser, C. (1983) "Real business cycles," *Journal of Political Economy*, Vol. 91, pp. 39–69.

Lucas, R. E. J. (1977) "Understanding business cycles," in *Carnegie-Rochester conference series on public policy*, Vol. 5, pp. 7–29, North-Holland.

Matsuyama, K. (1999) "Growing through cycles," *Econometrica*, Vol. 67, pp. 335–347.

——— (2007) "Credit traps and credit cycles," *American Economic Review*, Vol. 97, pp. 503–516.

Matsuyama, K., Sushko, I., and Gardini, L. (2014) "Globalization and synchronization of innovation cycles."

Miller, R. E. and Blair, P. D. (2009) *Input-output analysis: foundations and extensions*: Cambridge University Press.

Nakao, H. (2016) "Phase reduction approach to synchronization of nonlinear oscillators," *Contemporary Physics*, Vol. 57, pp. 188–214.

Ng, E. C. (2010) "Production fragmentation and business-cycle comovement," *Journal of International Economics*, Vol. 82, pp. 1–14.

Nikolaidi, M. and Stockhammer, E. (2017) "Minsky models: A structured survey," *Journal of Economic Surveys*, Vol. 31, pp. 1304–1331.

Pangallo, M. (2019) "Endogenous fluctuations in game theory and macroeconomics," Ph.D. dissertation, University of Oxford.

Pecora, L. M. and Carroll, T. L. (1990) "Synchronization in chaotic systems," *Physical Review Letters*, Vol. 64, p. 821.

——— (1998) "Master stability functions for synchronized coupled systems," *Physical Review Letters*, Vol. 80, p. 2109.

Pikovsky, A., Kurths, J., Rosenblum, M., and Kurths, J. (2003) *Synchronization: a universal concept in nonlinear sciences*, Vol. 12: Cambridge University Press.

Rodrigues, F. A., Peron, T. K. D., Ji, P., and Kurths, J. (2016) "The Kuramoto model in complex networks," *Physics Reports*, Vol. 610, pp. 1–98.

Rosenblum, M. G., Pikovsky, A. S., and Kurths, J. (1996) "Phase synchronization of chaotic oscillators," *Physical Review Letters*, Vol. 76, p. 1804.

Scheinkman, J. A. and LeBaron, B. (1989) "Nonlinear dynamics and stock returns," *The Journal of Business*, Vol. 62, pp. 311–337.

Selover, D. D. and Jensen, R. V. (1999) "Mode-locking and international business cycle transmission," *Journal of Economic Dynamics and Control*, Vol. 23, pp. 591–618.

Shintani, M. and Linton, O. (2004) "Nonparametric neural network estimation of Lyapunov exponents and a direct test for chaos," *Journal of Econometrics*, Vol. 120, pp. 1–33.

Shleifer, A. (1986) "Implementation cycles," *Journal of Political Economy*, Vol. 94, pp. 1163–1190.

Silverberg, G. and Lehnert, D. (1993) "Long waves and "evolutionary chaos" in a simple Schumpeterian model of embodied technical change," *Structural Change and Economic Dynamics*, Vol. 4, pp. 9–37.

Strogatz, S. (2004) *Sync: The emerging science of spontaneous order*: Penguin UK.

Timmer, M. P., Dietzenbacher, E., Los, B., Stehrer, R., and De Vries, G. J. (2015) "An illustrated user guide to the world input–output database: the case of global automotive production," *Review of International Economics*, Vol. 23, pp. 575–605.

Watts, D. J. and Strogatz, S. H. (1998) "Collective dynamics of "small-world" networks," *Nature*, Vol. 393, p. 440.

A Construction of the dataset

To empirically analyze the synchronization of disaggregate endogenous business cycles, it is necessary to build a dataset of the main macroeconomic variables that spans as many years, sectors and countries as possible. These dimensions usually involve a tradeoff: very disaggregate datasets are only available in a few countries for at most the last 30 years, while datasets that go further back tend to be very aggregate (i.e. have at most a few macro sectors).

This appendix describes the creation of a dataset that strikes a compromise between the best coverage on the year, sector and country dimensions. The final dataset covers six main macroeconomic variables (employment, hours worked, investment, gross output, GDP, inflation)—we only use employment and real GDP in the main paper, but we plan to extend our analysis to other variables—, 17 countries, 37 sectors and the years between 1960 and 2016, for a total of 215,118 data points. This dataset is obtained by merging six databases: KLEMS, OECD STAN 3, OECD STAN 4, UNIDO INDSTAT 2, OECD ISDB and GGDC 10-sector. All these "source" datasets miss some variable/country/sector/year combinations. For example, KLEMS, which has highest data availability among the source datasets, only covers around 65% of the potential data points. Merging these datasets increases data availability to 84%.

Of course merging requires making additional assumptions, which in some cases can be problematic. This section describes the final dataset and discusses the assumptions that had to be made to compare and harmonize the source datasets.

A.1 Source datasets

Sectoral macroeconomic data are available in a variety of datasets. Here we focus on six databases that strike a balance between the requirements described above: length of the time series and country and sector coverage. The databases we focus on are the following.

Table 3: Source databases.

Name	Countries	Sectors	Temporal span	Variables
KLEMS	All	All (ISIC 3)	1970-2007	All
STAN3	All	All (ISIC 3)	1970-2009	All
STAN4	All	All (ISIC 4)	1995-2016	All
ISDB	All but Spain, Portugal, Austria, Ireland	All but L-M-N-O-P (ISIC 3)	1960-1995	All but gross output and hours worked
UNIDO	All	Only manufacturing (ISIC 3)	1963-2016	All but inflation and hours worked
GGDC	All but Canada, Australia, Portugal, Austria, Belgium, Ireland, Finland	10 macro-sectors (AtB, C, D, E, F, GtH, I, JtK, LtN, OtP), ISIC 3	1960-2011	Employment, GDP, inflation

All countries: US, Canada, Japan, Australia, EU (UK, France, Germany, Italy, Spain, Portugal, Austria, Belgium, Ireland, Netherlands, Sweden, Finland, Denmark);
All sectors: ISIC rev. 3, 2-digit sectors and aggregates thereof. See Table 7 for a complete list;
Relevant temporal span: 1960-2016;
All variables: employment, hours worked, investment, gross output, GDP, inflation.

A.1.1 KLEMS

The KLEMS[29] (Kapital, Labor, Energy, Materials, Services) has been developed first in Europe (EU KLEMS) and then in other countries (WORLD KLEMS) to study issues related to outputs, inputs and productivity at a relatively detailed sectoral level. KLEMS covers several developed and developing countries. Coverage in terms of variables, years and sectors is highly heterogeneous. For the countries we focus on, variables are mostly available 1970-2007, for about 27 basic sectors and aggregates thereof. We mostly use the latest vintages of KLEMS data that are available in ISIC (International Standard Industrial Classification) rev. 3. KLEMS has all employment, hours worked, investment (not in all countries), output, GDP and inflation variables.

A.1.2 STAN3 and STAN4

The STAN[30] (STructural ANalysis) database has been developed by the OECD "to analyze industrial performance at relatively detailed level across countries". It is similar to KLEMS in terms of coverage and primary sources. Here we use two vintages of STAN, based on two different ISIC classifications. We will name STAN3 the version of STAN that is based on ISIC rev. 3, and available 1970-2009, and STAN4 the version based on ISIC rev. 4, available mostly 1995-2016. Both STAN3 and STAN4 have the same variables as KLEMS (employment, hours, investment, output, GDP and inflation).

A.1.3 ISDB

The ISDB[31] (International Sectoral DataBase), also developed by the OECD, is a precursor of STAN. Availability is 1960-1995 for most countries considered here (ISDB was discontinued in 1995, and replaced by STAN). The sectoral coverage (ISIC rev.3) is similar to KLEMS and STAN, but some sectors in services are not available. Gross output and sectoral hours worked are not available, while all other variables are available.

A.1.4 UNIDO

The UNIDO[32] (United Nations Industrial Development Organization) INDSTAT 2 database is maintained by the UN and is "particularly valuable for long-term structural analysis". It only covers manufacturing sectors (ISIC rev.3), for the period 1963-2016, for most countries in the world. It has the same variables as the other datasets, except hours worked and inflation.

A.1.5 GGDC

The GGDC[33] (Groningen Growth and Development Center) 10-sector database is maintained by the GGDC and is also meant to study long-run sectoral productivity performance. It contains 10 aggregate sectors (ISIC rev. 3), for the period 1950-2011, for several developed and developing country. The only available variables are total employment, GDP and inflation.

A.2 Harmonized dataset and data processing

The datasets described in the previous section are in many cases complementary, in the sense that some country/sector/variable/year combinations may be available in one dataset

[29] Data downloaded from `http://www.euklems.net/` and `http://www.worldklems.net/data.htm`.

[30] Data downloaded from `http://stats.oecd.org/wbos/Index.aspx?DatasetCode=STAN08BIS&lang=en` and `http://stats.oecd.org/Index.aspx?DataSetCode=STANI4_2016`.

[31] Data downloaded from `http://fmwww.bc.edu/ec-p/data/isdb.html`.

[32] Data described at `https://stat.unido.org/content/dataset_description/indstat-2-2018%252c-isic-revision-3` and obtained through UK Data Service.

[33] Data downloaded from `https://www.rug.nl/ggdc/productivity/10-sector/`.

but not in others. Motivated by this, we create a *harmonized dataset* that complements the missing combinations. As we will see, for each variable we will get at least 20% more data points than if we just used the single dataset with most data points (KLEMS). This harmonized dataset comprises:

- Six variables: employment, hours worked, investment, output, GDP and inflation. Employment is in thousands of employed workers (employees+self-employed); hours worked is given in millions of hours; investment, output and GDP are given in millions of current values of local currencies; inflation is obtained from GDP at constant prices (base year = 2005), by calculating the sectoral GDP deflator (the actual data in the dataset are the sectoral price indexes rather than inflation rates). These are the business cycle variables that are most relevant for sectoral analysis. For example, consumption is only relevant to the sectors whose output is mostly consumed; however, for some manufacturing sectors the output is almost totally invested. Nevertheless, it would be desirable in the future to add other variables, such as inventories, capital stock, financial variables, wages, exports, imports, etc.
- 57 years: 1960-2016. Data from 1950 are only available in a small subset of countries. In addition, recovery from WWII may create spurious results. 2017 and 2018 are not yet available.
- 17 countries: US, Canada, Japan, Australia, EU (UK, France, Germany, Italy, Spain, Portugal, Austria, Belgium, Ireland, Netherlands, Sweden, Finland, Denmark). These are a selection of large, medium and small countries that had a similar development in the period analyzed and so can be compared most trustfully. The selection of these countries is however mainly driven by data availability (developing countries only have had reliable data for at most 30 years).
- 37 sectors: 27 basic sectors (agriculture, mining, 11 manufacturing, utilities, construction, 13 services) and 10 aggregates thereof. This seems to be the best compromise between detail of sectoral disaggregation and data availability. For a full list of sectors, see Table 7.

In practice, the creation of the dataset proceeds in the following two steps.

A.2.1 Comparison

To properly compare the different datasets, sectors must be made compatible. This is trivial for the ISIC 3 datasets, as it is enough to give the same name to the same sectors in the different databases and then join the data. It is much less obvious to map ISIC 4 quantities to the corresponding ISIC 3 aggregates. There exist concordance tables, but these are based on 4-digit classifications, while we only have 2-digit sectors. After some experimentation, it seemed best to manually map ISIC 4 quantities to ISIC 3 aggregates. For example, there exists a ISIC 3 sector named "21t22 - Pulp, paper, paper products, printing and publishing". According to our manual mapping, this is obtained summing the ISIC 4 sectors "17 - Paper and paper products", "18 - Printing and reproduction of recorded media" and "58 - Publishing activities". This manual mapping is adjusted depending on data availability. While this choice is not optimal, we manually check all mappings and in most cases the trends of the aggregated ISIC 4 sectors closely correspond to those of the corresponding ISIC 3 sectors over the overlapping years. If some ISIC 4 sectors are not available (e.g. "58 - Publishing activities" is not available for many countries/variables), in most cases we give up using the ISIC 4 data. Unfortunately, absent guidance from the statistical agencies that created the primary databases, we could not find other alternatives.

Another necessary step at this stage is to harmonize the units in which variables are measured. For instance, some datasets measure variables in thousands of units while other datasets provide data in millions of units. Moreover, investment, gross output and GDP are given in current prices of local currency. Since ISDB stops in 1995, this local currency does not correspond to the euro, which was adopted by several countries starting from 1999, so conversion to euro is necessary. Finally, constant price GDP (used to calculate producer price indexes and so sectoral inflation rates) often has different base years. Given that finding, a common year to rebase GDP would lead to data loss, we do not rebase them to the same year, given that in this case the harmonization procedure discussed in the next section does not require it.

A.2.2 Harmonization

During certain years, only some of the datasets are available. For example, in the period before 1970 only GGDC, UNIDO and ISDB are available, and after 2010 only STAN4 and UNIDO are often available. Therefore, starting from a dataset that is reliable and available in the intermediate years for all sectors/countries, we extend this dataset to cover the initial and final years. The algorithm is as follows:

1. Choose a primary database that is reliable and almost always available, at least in the intermediate years. In almost all cases this is KLEMS, in a few cases it is STAN3.
2. For the initial and final years, extend this dataset with the longest available dataset. When there is more than one dataset with the same availability, the algorithm selects the time series with highest correlation with the basic dataset.

Sometimes we join on levels, by adding a constant offset. An alternative is to keep constant growth rates, i.e. join the series logarithmically. That is, letting x_t denote the basic series (here KLEMS), y_t the other series (here STAN4), and $t = T$ the joining year (here $t = 2007$), a constant offset means defining a series $\tilde{y}_t$ such that

$$\tilde{y}_t = y_t + (x_T - y_T) \tag{22}$$

while logarithmic joining means considering a series $\hat{y}_t$

$$\hat{y}_t = \exp\left(\log\left(y_t\right) + \left(\log\left(x_T\right) - \log\left(y_T\right)\right)\right). \tag{23}$$

No solution is superior a priori: $\tilde{y}_t$ preserves levels, while $\hat{y}_t$ preserves growth rates. We use the former for labor market variables, employment and hours worked, and the latter for "currency variables", investment, output, GDP and inflation. For inflation (obtained from constant price GDP), using logarithmic joining is particularly useful as it does not require that price indexes coming from different datasets have the same base year, since growth rates are invariant to the choice of the base year.

A final problem with the harmonization procedure is that aggregates may be inconsistent, that is they do not correspond to the sum of subsectors. This is due to several causes:

1. Aggregates may be inconsistent in the original data
2. Inconsistencies can be created by joining different datasets. For example, if one joins aggregate manufacturing in the final years with the STAN4 data but joins some manufacturing subsectors with UNIDO data, the sum of the manufacturing subsectors need not match aggregate manufacturing.
3. Inconsistencies can be created with the logarithmic joining, Eq. (23). Given $z_t = x_t + y_t$, it is generally the case that $\hat{z}_t \neq \hat{x}_t + \hat{y}_t$. This is due to preserving growth rates instead of levels.
4. In the case of constant price GDP, rebasing to a different years also creates aggregation inconsistencies. In formula, letting x_t^T denote a variable at time t with base year T, even if $z_t^T = x_t^T + y_t^T$, it is usually $z_t^{T'} \neq x_t^{T'} + y_t^{T'}$.

Therefore, all aggregates are computed again after joining and harmonizing the different datasets.

A.3 Final data availability

All this work allows to recover about 84% of the data that cover the period 1960-2016, for 17 countries, 37 sectors and 6 variables (total 215,118 data points). Table 4 shows the comparison with the other datasets, both across all variables and for each variable. Across all variables, the second dataset with highest data availability is KLEMS, with 65%. Therefore, the procedure described in these notes allows to recover about 20% more data than would have been possible by only using any single dataset. This percentage increases to about 30% in the case of investment.

Tables 5, 6 and 7 disaggregate data by years, countries and sectors respectively. These suggest that much of the lack of data is due to the 1960-1969 period, that coverage is quite uniform across countries, and that coverage is slightly larger in manufacturing than in services (because of UNIDO INDSTAT 2, which covers manufacturing only).

Table 4: Ratio of available data vs. all data (1960:2016, 17 countries, 37 sectors)

var	combined	KLEMS	STAN4	STAN3	UNIDO	ISDB	GGDC
tot	0.84	0.65	0.53	0.47	0.19	0.16	0.07
emp	0.89	0.68	0.59	0.56	0.30	0.23	0.14
hours	0.80	0.69	0.44	0.25	0.00	0.01	0.00
inv	0.80	0.49	0.52	0.50	0.26	0.24	0.00
output	0.84	0.68	0.54	0.48	0.30	0.00	0.00
gdp	0.88	0.68	0.58	0.56	0.29	0.25	0.13
gdpconst	0.85	0.68	0.54	0.47	0.00	0.24	0.15

Table 5: Ratio of available data vs. all data (all variables, 17 countries, 37 sectors)

year	combined	KLEMS	STAN4	STAN3	UNIDO	ISDB	GGDC
1960-2016	0.84	0.65	0.53	0.47	0.19	0.16	0.07
1960-1969	0.35	0.10	0.00	0.00	0.13	0.16	0.06
1970-1979	0.94	0.92	0.33	0.44	0.21	0.28	0.08
1980-1989	0.95	0.94	0.47	0.64	0.21	0.29	0.08
1990-1999	0.97	0.96	0.73	0.78	0.19	0.18	0.08
2000-2009	0.96	0.79	0.91	0.80	0.20	0.00	0.08
2010-2016	0.89	0.02	0.87	0.00	0.20	0.00	0.01

Table 6: Ratio of available data vs. all data (all variables, 1960-2016, 37 sectors)

country	combined	KLEMS	STAN4	STAN3	UNIDO	ISDB	GGDC
all	0.84	0.65	0.53	0.47	0.19	0.16	0.07
Australia	0.80	0.66	0.37	0.27	0.19	0.14	0.00
Austria	0.81	0.64	0.64	0.55	0.19	0.00	0.00
Belgium	0.81	0.55	0.44	0.47	0.18	0.17	0.00
Canada	0.94	0.83	0.55	0.52	0.18	0.23	0.00
Denmark	0.84	0.66	0.79	0.66	0.19	0.21	0.08
Finland	0.88	0.66	0.72	0.63	0.20	0.26	0.00
France	0.85	0.63	0.61	0.57	0.19	0.25	0.13
Germany	0.86	0.60	0.42	0.36	0.19	0.26	0.08
Ireland	0.79	0.55	0.39	0.26	0.19	0.00	0.00
Italy	0.85	0.66	0.57	0.61	0.19	0.22	0.13
Japan	0.81	0.63	0.49	0.39	0.20	0.16	0.14
Netherlands	0.85	0.66	0.71	0.54	0.20	0.18	0.13
Portugal	0.77	0.57	0.40	0.33	0.19	0.00	0.00
Spain	0.83	0.66	0.40	0.43	0.20	0.00	0.13
Sweden	0.83	0.60	0.54	0.48	0.19	0.19	0.13
UK	0.84	0.66	0.45	0.39	0.18	0.19	0.13
US	0.96	0.87	0.59	0.50	0.20	0.27	0.13

Table 7: Ratio of available data vs. all data (all variables, 1960-2016, 17 countries)

country	combined	KLEMS	STAN4	STAN3	UNIDO	ISDB	GGDC
all	0.84	0.65	0.53	0.47	0.19	0.16	0.07
TOT - TOTAL INDUSTRIES	0.91	0.67	0.72	0.55	0.00	0.34	0.23
AtB - Agriculture	0.89	0.66	0.70	0.54	0.00	0.28	0.23
C - Mining	0.89	0.66	0.69	0.48	0.00	0.25	0.23
D - TOTAL MANUFACTURING	0.93	0.66	0.49	0.57	0.61	0.29	0.23
15t16 - Food	0.92	0.66	0.63	0.54	0.50	0.27	0.00
17t19 - Textiles	0.92	0.66	0.62	0.54	0.61	0.27	0.00
20 - Wood	0.91	0.66	0.57	0.52	0.61	0.22	0.00
21t22 - Paper	0.91	0.66	0.43	0.52	0.61	0.26	0.00
23t25 - Chemical	0.90	0.66	0.56	0.53	0.53	0.27	0.00
26 - Non-metallic minerals	0.91	0.66	0.58	0.53	0.61	0.27	0.00
27t28 - Metal	0.91	0.66	0.63	0.53	0.61	0.18	0.00
29 - Machinery	0.90	0.66	0.62	0.46	0.59	0.00	0.00
30t33 - Electrical and optical equipment	0.91	0.66	0.62	0.46	0.59	0.14	0.00
34t35 - Transport equipment	0.91	0.66	0.63	0.54	0.59	0.20	0.00
36t37 - Manufacturing NEC	0.89	0.66	0.45	0.52	0.59	0.00	0.00
E - Utilities	0.88	0.66	0.51	0.54	0.00	0.29	0.23
F - Construction	0.89	0.66	0.69	0.54	0.00	0.29	0.23
G - Trade	0.86	0.66	0.49	0.47	0.00	0.27	0.00
H - Hotels and restaurants	0.86	0.66	0.60	0.47	0.00	0.23	0.00
GtH - TRADE, RESTAURANTS AND HOTELS	0.87	0.66	0.49	0.47	0.00	0.23	0.23
I - TRANSPORT AND STORAGE AND COMMUNICATION	0.86	0.65	0.43	0.53	0.00	0.28	0.23
60t63 - Transport and storage	0.83	0.66	0.46	0.44	0.00	0.23	0.00
64 - Communication	0.83	0.65	0.43	0.44	0.00	0.23	0.00
JtK - FINANCE, INSURANCE, REAL ESTATE AND BUSINESS SERVICES	0.88	0.66	0.52	0.53	0.00	0.24	0.23
J - Finance, insurance	0.86	0.66	0.60	0.49	0.00	0.24	0.00
K - REAL ESTATE AND BUSINESS SERVICES	0.85	0.66	0.52	0.48	0.00	0.20	0.00
70 - Real estate	0.82	0.66	0.57	0.38	0.00	0.00	0.00
71t74 - Other business	0.81	0.66	0.52	0.37	0.00	0.00	0.00
LtQ - COMMUNITY SOCIAL AND PERSONAL SERVICES	0.81	0.66	0.43	0.53	0.00	0.00	0.00
L - Public admin	0.82	0.66	0.58	0.45	0.00	0.00	0.00
M - Education	0.82	0.66	0.58	0.44	0.00	0.00	0.00
N - Health	0.82	0.66	0.59	0.45	0.00	0.00	0.00
LtN - GOVERNMENT SERVICES	0.85	0.66	0.57	0.44	0.00	0.00	0.23
O - Other services	0.80	0.66	0.45	0.44	0.00	0.00	0.00
P - Private households with employed persons	0.70	0.60	0.40	0.28	0.00	0.00	0.00
OtP - COMMUNITY, SOCIAL AND PERSONAL SERVICES	0.84	0.65	0.43	0.32	0.00	0.00	0.23
Q - EXTRA-TERRITORIAL ORGANIZATIONS AND BODIES	0.00	0.41	0.00	0.00	0.00	0.00	0.00

B Further correlation data

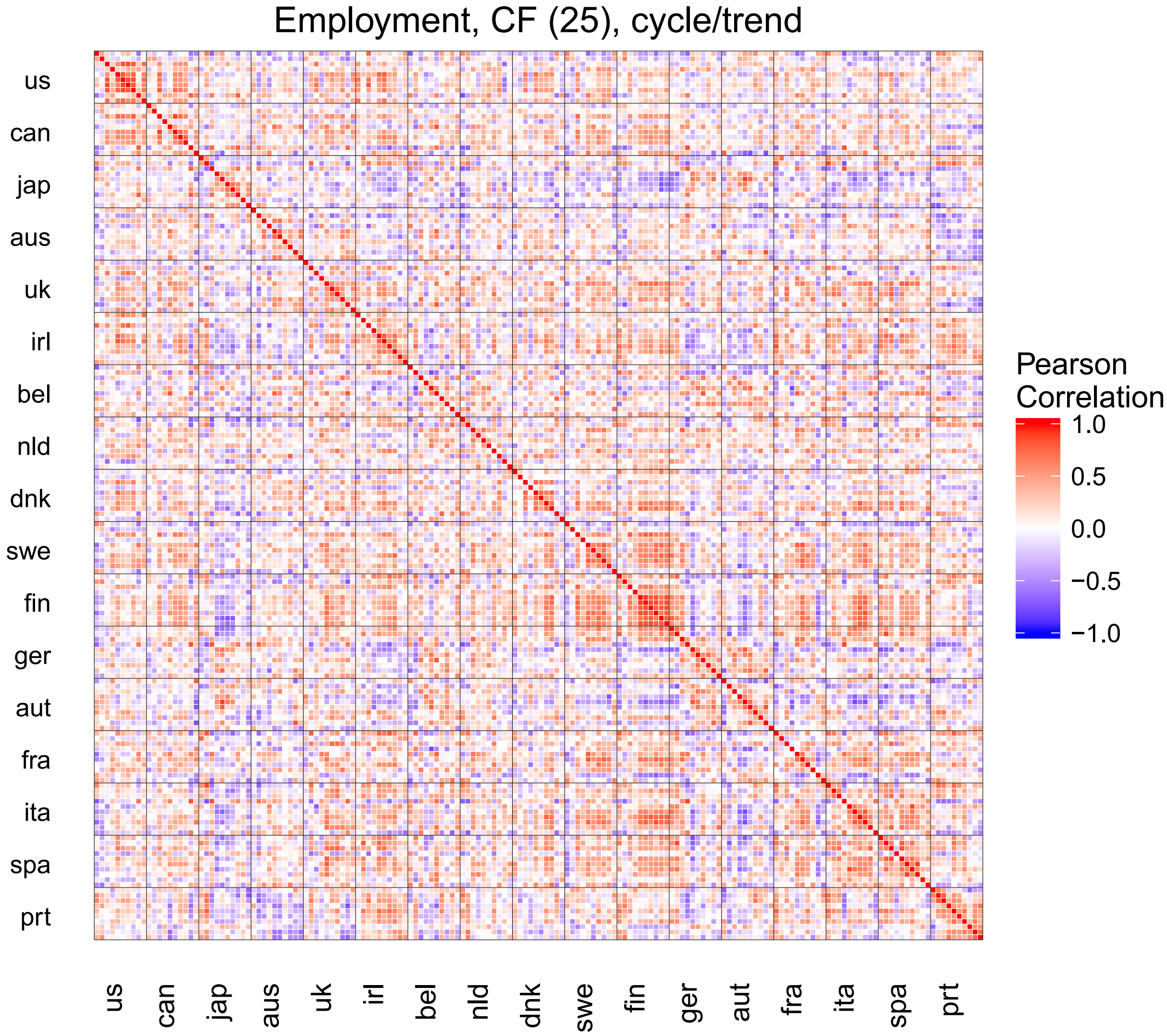

Figure 17: Pairwise Pearson correlation coefficients across all combinations of 10 aggregate sectors and 17 countries. Data are grouped by country; the order of sectors within each country is the same as in Figure 18. We detrend data with a CF(25) filter, and consider the ratio between cycle and trend.

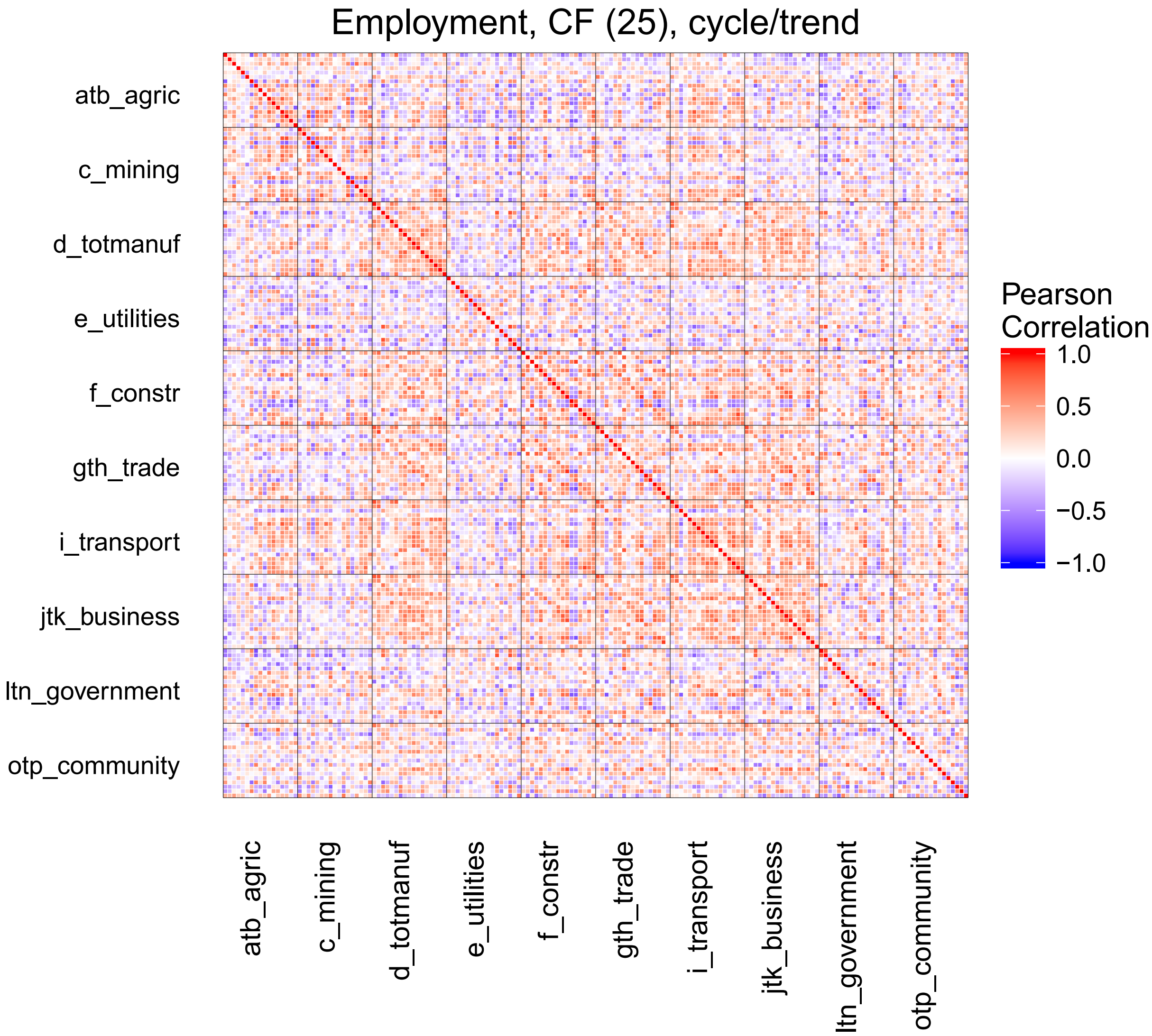

Figure 18: Pairwise Pearson correlation coefficients across all combinations of 10 sectors and 17 countries. Data are grouped by sector; the order of countries within each sector is the same as in Figure 17. We detrend data with a CF(25) filter, and consider the ratio between cycle and trend.